APPLIED PHYSICS REVIEWS

Electrical transport mechanisms in three dimensional ensembles of silicon quantum dots

I. Balberg[a)]
The Racah Institute of Physics, The Hebrew University, Jerusalem 91904, Israel

(Received 16 May 2011; accepted 22 August 2011; published online 29 September 2011)

In this review, we try to derive a comprehensive understanding of the transport mechanisms in three dimensional ensembles of Si quantum dots (QDs) that are embedded in an insulating matrix. This understanding is based on our systematic electrical measurements as a function of the density of Si nanocrystallites as well as on a critical examination of the available literature. We conclude that in ensembles of low density QDs, the conduction is controlled by quantum confinement and Coulomb blockade effects while in the high density regime, the system behaves as a simple disordered semiconductor. In between these extremes, the transport is determined by the clustering of the QDs. In view of the clustering, two types of transitions in the electrical and optical properties of the system are identified. In order to understand them, we introduce the concept of "touching." The application of this concept enables us to suggest that the first transition is a local carrier deconfinement transition, at which the concentration of the non "touching" QDs reaches its maximum, and that the other transition is associated with the onset of percolation in a continuous disordered network of "touching" QDs. It is hoped that our conclusions for the entire possible density range will provide guidance for the discussion and understanding of the transport in ensembles of semiconductor QDs in general and in ensembles of Si and Ge QDs in particular. © *2011 American Institute of Physics*. [doi:10.1063/1.3637636]

TABLE OF CONTENTS

I. INTRODUCTION

While the optical properties of solid ensembles of semiconductor quantum dots have been studied intensively,[1,2] the understanding of their transport properties is still at initial stages.[2,3] The purpose of this review is to provide then a framework for the discussion of the transport in such systems by considering systematically phenomena in a system for which few data already exist but for which a comprehensive discussion has not been given yet. The system that we studied for that purpose is that of Si nanocrystallites (NCs) embedded in an insulating matrix.[2,4,5] While memory-charge storage (CS) characteristics of two dimensional (2D) arrays of Si NCs have been intensively investigated,[6] relatively little attention was given to the transport in 3D ensembles of such quantum dots (QDs).[4] However, the transport in the latter systems is expected to yield new basic physics as well as potential applications. In particular, we expect that in addition to the present reasonable[7] understanding of the transport in granular metals,[8] new significant insights as well as new phenomena will be found in semiconductor QDs, following the presence of discrete (confined[1] or other typical semiconductor-like[9]) levels. Primarily, one would expect that the combination of Coulomb blockade (CB) and quantum confinement (QC) restrictions may yield various resonant tunneling effects[10] as well as various quantum phase transformations.[11] From the possible applications point of view, we should mention the above memories,[6] the solar cells[12] and the light emitting diodes (LEDs).[13] In all of these, significant performance can come about only in dense enough 3D ensembles of semiconductor NCs that must have efficient transport in them.[13,14]

Turning to the transport in 3D ensembles of Si QDs, we note that the main results obtained on lower dimensional ensembles of Si QDs (i.e., 0D-like,[15] 1D-like,[15,16] or

[a)]Author to whom correspondence should be addressed. Electronic mail: balberg@vms.huji.ac.il.

perpendicular to 2D arrays[17–19]) provide a reference for the discussion of the transport in ensembles of larger dimensions. The interpretation of those results followed the basic physics of the CB (Ref. 10) and the QC (Refs. 1 and 2) in single-isolated NCs.[20] Correspondingly, the understanding of the electronic properties of the single isolated NC is quite necessary in order to interpret the transport data in ensembles[21–23] of semiconductor NCs. Noting, however, that reviews on the electrical properties of essentially isolated NCs are available,[5,15] we mention here only the presently relevant highlights of these studies. It turns out that the knowledge we have on the level separation in Si quantum dots comes almost exclusively from optical measurements[2,24] and the corresponding results are reasonably accounted for by relatively simple theoretical models.[2,25,26] On the other hand, the determination of the electronic structure by local electrical measurements[15] that are more relevant to the studies of the transport properties via semiconductor quantum dots, is much less conclusive in the case of Si NCs than in other (say, CdSe NCs) systems.[27] Considering the many difficulties associated with the interpretation of the results obtained for Si NCs, the best information that could have been deduced from them is that the confined level separations and the CB energy are of the order of 0.1-0.3 eV when the NCs are in the 3-5 nm-size regime.[15] Also, charge induced by electrical force microscopy (EFM) has been used by a few groups[28–30] to demonstrate that individual Si NCs can be charged if they are well removed from each other. Probably, a better defined system for electrical spectroscopy of isolated Si NCs is the structure where only a couple of Si-NCs are present between two contacts.[15,16] Such a system yields a well defined double barrier tunnel junction (DBTJ)-like configuration that is reminiscent of the DBTJs that were studied in systems of II-VI and III-V NCs.[27,31,32] While the above studies of "isolated" Si NCs do not provide a comprehensive and/or unified model for the values of the Coulomb blockade and quantum confinement energies, E_{CB} and E_{QC}, in the Si NC, we shall assume below that, as in the II-VI and III-V semiconductors, the two effects play an important role in the transport between the Si NCs in their ensembles.[20] While not established in detail, the above conclusion can be considered as properly founded and generally accepted.

Following the above, let us define briefly the basic concepts that we mentioned above in the context of the single-isolated QDs. The separation between the energy levels that lie within the bulk's energy-band range and that result from QC is given (roughly) by[1,2]

$$E_{QC} \propto 1/m * d^2, \tag{1}$$

where d is the diameter of the QD and m* is an "effective" effective mass i.e., the effective mass[9] that can be deduced from the calculated or measured electronic structure of the QD in the corresponding quantum well configuration.[25,33] As a first approximation, it is common[20,26,34] to use the bulk effective mass (which is, in units of the free electron mass, 0.3 for electrons and 0.5 for holes in crystalline Si[20,26]). In order to get a carrier tunneling between two NCs, we need a matching of the two ground (or upper lying) states[21,27] or we "need to provide" the energy differences between their E_{QC} values (by field or thermal excitation) as in the well known hopping process.[35] This process is known as resonant tunneling[31] between two NCs, and its manifestation in the entire macroscopic system of NCs is known as sequential resonant tunneling.[4,21] Considering the electrostatic charging effect, we note that the transfer of an electron from a given neutral particle to an adjacent neutral particle brings about the charging of the original particle by one positive elementary charge (q) and to the charging of the adjacent particle by one negative elementary charge.[8] If the capacitance of an individual particle in its corresponding environment is C_0, the energy needed to be supplied for the above "electron-hole" transfer by tunneling is the Coulomb blockade energy[4,8,10]

$$E_{CB} = q^2/C_0. \tag{2}$$

Of course in the simplest case of an isolated sphere, $C_0 = 2\varepsilon\varepsilon_0 d$, where $\varepsilon\varepsilon_0$ is the dielectric constant of the insulating matrix. Following the above discussion (Eqs. (1) and (2)), we can conclude that the energy needed for the "hopping" between two semiconductor NCs can be expressed, to first order, by[4,21,27,34,36]

$$E = E_{CB} + \Delta E_{QC}, \tag{3}$$

where, ΔE_{QC} is the energy difference between the "conducting" levels in adjacent NCs. This energy difference may arise from different d's, or different potential wells that are caused, for example, by different QDs environments, such as different distances between the QDs.

Unlike the lower dimensional ensembles,[5,15,16] the electrical transport in ensembles of 3D systems of Si NCs has not been studied intensively and no comprehensive picture of the electrical conduction in them was suggested. While a more detailed critical description of previous studies of these systems will be given in Sec. III, let us mention already here the difficulty to deduce such a comprehensive understanding from the available literature. The foremost conspicuous drawback in the majority of previous studies is the lack of correlation between the geometrical structures of the ensembles and/or the density, N, of the NCs in them, with the interpretation of the transport data. Correspondingly, usually only a single macroscopic transport measurement on one ensemble was taken and the result was interpreted as due to a particular transport mechanism that was or was not consistent with the structure of the ensemble. The other conspicuous drawback was that in the majority of studies, the transport mechanism was deduced solely from the temperature dependence of the dark conductivity, $\sigma(T)$. Since, the studied samples were of relatively high resistance, the temperature range over which it was possible to carry out the measurements was relatively narrow and thus, the analyses presented cannot be considered conclusive.[35] These two drawbacks caused most researchers to suggest that the transport mechanism in their samples is "hopping," without specifying whether the hopping is between the NCs or between some other entities, such as defects, in the system. Obviously, without knowing the

value of N, this conclusion of "hopping" is not meaningful. While this was usually the case for systems where it was a priori assumed that N is relatively small, the mechanism of thermionic emission[37] has been usually suggested for systems where N was assumed a priori to be very high.[15,38] The fact that the suggested semiconductor-barriers have little meaning (there is on the average only a single "free" electron per NC) has been ignored. These problems have been overlooked, even in recent reviews[15] where no attention was given to the importance of the density of the NCs. Correspondingly, it appears to us that the very popular σ(T) data by itself may yield questionable interpretations. As we discuss in this work, this is not only the case for the σ(T) data but also for the other popular type of data that comes from the measurement of the current voltage (I-V) characteristics. Hence, again, the derived I(V) dependence and its interpretation are not unique, when no other supporting data are provided.

Considering the above background, we will try to present below probably the first comprehensive critical review of the works on the transport in ensembles of Si NCs embedded in an insulating continuous matrix by adding (to the commonly studied σ(T) and I-V dependencies) the very important information on the density of the NCs. We shall attempt to show that this parameter provides a very useful scale along which one can follow the basic transport mechanisms in 3D ensembles of NCs. In particular, we shall emphasize the importance of the system-connectivity that has hardly been discussed in the past.[14] This is in contrast with the inter-dot tunneling aspect of the transport that was emphasized previously.[15] We should mention here that the need to consider the connectivity as well as the intercrystallite charge transfer was first recognized by Burr *et al*. in 1997,[14] while the first consideration of the density of the ensembles of Ge NCs was that of Fujii *et al*. in 1999.[21] These two works may be viewed as the major pioneering works on the transport in 3D ensembles of column IV semiconductor NCs. Following the above background, our approach to gain a comprehensive understanding of the above transport problem was then to study the σ(T) and I(V) dependencies as a function of the density of the NCs. This approach enables us to analyze the various transport data beyond the very dilute NCs range where granular-metal-like hopping conduction[7,8,39,40] is probably the only possible transport mechanism. We will see that the combination of the "hopping" mechanism and the conduction between "touching" NCs (to be accurately defined below) are then the "corner stones" of the description of the transport in ensembles of semiconductor quantum dots. In order to achieve this conclusion, we have studied a variety of well characterized structures of Si-NCs ensembles. This enabled us to reduce the number of the possible scenarios that can account for the experimental data.

In comparing the results of our own work with the relevant works of others, we limited ourselves in this review to ensembles where the Si NCs are smaller than 10 nm, since for these NCs both, the QC and CB effects become significant even at room temperature.[13,20,24] We note in passing that in the literature, the term Si NCs has been used frequently for much larger particles that do not exhibit quantum confinement and/or charging effects[41–43] and these will not be reviewed here. Also, we do not discuss here the ensembles of Si NCs that are embedded in a disordered Si tissue as in porous silicon. The transport in the latter system that has been considered previously by us[4,44] and by others[2,45] is quite different from that in the systems discussed here since, in contrast with the systems of present interest, the disordered Si matrix in porous silicon provides current routes that are parallel to those controlled solely by the Si NCs network. Also, in order to limit the scope of this review, we will not give an extended literature list of the relevant theories and experimental results but we will refer to works that we found essential for providing the comprehensive picture that we attempt to derive. We believe however that quite a full account of the works in the field can be found in the literature that is cited here.

The present review is structured as follows. In Sec. II, we describe our method of sample-fabrication and the structural, electrical, and optical characterization of the samples that enabled us to evaluate the combined effects of inter-NCs conduction and connectivity on the transport in the system. Then, in Sec. III, we present our experimental results that emphasize the great importance of knowing the structure of the 3D system as the first step for a proper interpretation of the transport properties. We start that section by a brief review of our previous works.[46,47] In particular, we discuss the low density regime of the QDs ensembles (Sec. III A) in order to set the stage for the evaluation of the transport in the higher density regimes. This is followed by a detailed description of the other extreme i.e., of the very high density regime (Sec. III B) which enables us to suggest the concept of "touching" of NCs which we found to be essential for the understanding of the transport in all, but the extreme low density, regimes. The utilization of this concept and the inclusion of the charging-dominated effects will enable us then to suggest the corresponding transport mechanisms in the high (Sec. III B) and intermediate (Secs. III C–III E) NCs density regimes. We believe that the results that we review and their interpretation give an initial comprehensive framework for the discussion of the transport mechanisms in 3D ensembles of Si NC's. In Sec. IV, we describe and justify the conclusions that we derived from our experimental results, in a broader context and we show that, while we were able to obtain a comprehensive picture of the transport mechanisms in 3D ensembles of Si NCs, we are still far from the understanding of the transport in detail and/or from accounting quantitatively for most of the experimental observations of others and ours. Finally, in Sec. V, we present our main conclusions regarding the transport in these ensembles in a form that provides a framework for future discussion of that transport.

II. SAMPLE PREPARATION AND MEASUREMENT TECHNIQUES

In order to follow the effect of the NCs density on the behavior of the transport, we have applied in our studies probably the most suitable sample fabrication technique for such studies, i.e., the co-sputtering technique that is well

reviewed in the literature.[8,48] This is since the flexibility of this method provides solid films with a continuous variation of nano-particle densities that are fabricated under exactly the same conditions. We note that while many groups have applied the sputtering technique for the deposition of Si/SiO_2 films and some have applied it for obtaining a few Si-phase volume contents,[21] we do not know of any other group that applied this technique for obtaining such films with a continuous partial volume content, x, as a parameter. Using this versatility enabled us to carry out a systematic study of the optical[54] and electrical[46,47] properties as a function of the NCs density in a manner that has been previously applied only to granular metals.[8,48] We have co-sputtered then Si/SiO_2 films by utilizing two separate sources (targets)[50,51] One target was a high purity (99.999%) sintered silicon pellet or electronic quality Si wafer and the other consisted of pure (99.995%) fused quartz. The Si wafers (used for the study of doping effects) were n-type crystals with resistivities of 0.005, 0.1-0.5, and 20-30 Ω cm or p-type crystals of resistivities 0.015 and 20-30 Ω cm. The substrates that we used were typically, 13 cm long, 1 cm wide, and 0.7 mm thick quartz slides (for the transport measurements) or 0.3 mm thick slices of Si crystals that were cut out from Si wafers (for capacitance measurements). For the sputtering process, a substrate was positioned 6 or 12 cm above the line connecting the centers of the two targets and parallel to it.[50,51] The deposition conditions in our studies were not too different from those used in the studies of granular metal systems[8] and in other works on $Si-SiO_2$ composites.[52] For example, we have used Ar gas for generating the ions that bombard the targets, the base pressure in the vacuum chamber was typically 5×10^{-6} Torr, the rf power was 60 W (for each target) and the radio frequency (rf) was 12.56 MHz. The voltages measured on the targets during sputtering were about −250 V, on the Si target, and about −400 V, on the SiO_2 target.

Since the key advantage in our works was the ability to study Si NCs ensembles with continuous variations of the NCs density[50,53] and the NCs size,[53–55] we elaborate here somewhat on the determination of these parameters in our samples. In general, following a couple of hours of deposition, the substrate became coated with a film that was about 1 μm thick. The film so prepared is a mixture of Si and SiO_2, and since these two phases are immiscible a composite of the two phases forms. The film obtained was Si-phase rich at one end of the elongated substrate (the one close to the Si target) and SiO_2 rich at its other end.[46,47,53–57] Our Raman scattering, infra red (IR) spectroscopy, and x-ray diffraction (XRD) measurements confirmed that our films consist of amorphous SiO_2 and amorphous silicon (a-Si).[50] For the determination of the relative volume contents of the two phases along the co-sputtered film, two additional films, one of each phase, were sputtered under the same conditions. The comparison of the thicknesses of the three films along the substrate slide has enabled then the direct determination of the volume content of each of the two phases in the co-sputtered films. This is a very common procedure for the determination of the metallic volume content in granular metals.[8,48] As others,[52] we also found,[50] by infrared spectroscopy, that this procedure is amenable for the determination

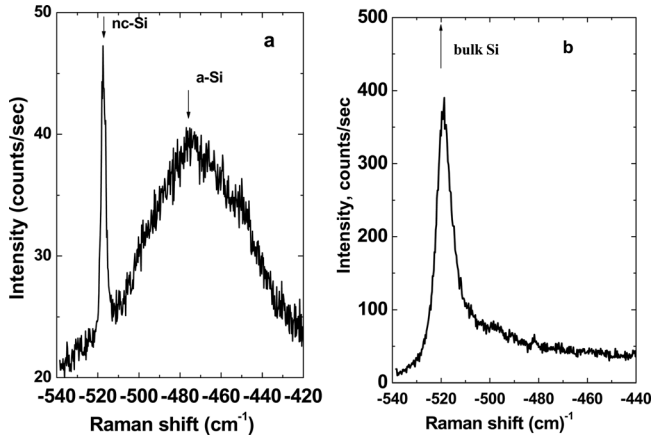

FIG. 1. Raman spectra of a co-sputtered film with x ≈ 75 vol. % before (a) and after (b) annealing. Reprinted with permission from N. Karpov, V. Volodin, J. Jedrzejewski, E. Savir, I. Balberg, Y. Goldstein, T. Egewskaya, N. Shwartz, and Z. Yanovitskaya, J. Optoelectron. Adv. Mater. 11, 625 (2009). Copyright © 2009, Wiley.

of the content of the SiO_2 phase and thus the fractional volume content of the Si phase, x. The latter quantity, at a given position along the substrate, was our characterization parameter of the Si phase content throughout this study. In our studies, we have monitored the variation of the various properties as a function of the position along the substrate yielding then their dependence on the value of x in terms of volume %.

Since the Si phase within the as-sputtered films was a-Si, we had to anneal the samples in order to generate Si NCs in the composite. After annealing (at 1150-1200 °C for a typical duration of 40 min, under a flow of 4 l/min of pure N_2), we reapplied the above structural characterization methods and added to them high resolution transmission electron-microscopy (HRTEM) measurements. We have carried out, in particular, a comprehensive study of the $Si-NCs/SiO_2$ ensembles by cross sectional HRTEM.[53,54] As shown in Fig. 1, we found from Raman scattering measurements that while some small amounts of silicon NCs are present in the non-annealed $a-Si/SiO_2$ samples, no a-Si is detectable in the annealed samples.[50] Also the analyses of the results of the above structural-determination methods revealed that the annealed films consist of amorphous SiO_2 and Si NCs.[53,54] We have determined the NCs size dependence on x or on the density of the NCs, $N = 6x/(100\pi d^3)$, where d is the "average" diameter of the crystallite. In the rest of the paper, d is defined as the value of crystallites' diameter at the peak of their Gaussian distribution. Such a distribution with d = 4 nm is shown in Fig. 2. We found that the typical d values were around 3 nm, at the Si poor end of the films, and around 10 nm, at the Si rich end of the films.[53–55] One can approximate the dependence of d on x by $d = d_0(x\text{-}x_0)^{1/3}$ where d_0 and x_0 depend on the fabrication conditions.[53] Typically, however in our samples, $d_0 \approx 2$ nm and $x_0 \approx 8$ vol. %.

In order to carry out the electrical measurements, we have provided electrical contacts as follows. For the films deposited on quartz substrates, we have used sets of sputtered aluminum or silver electrodes, 1 mm wide (0.2 to 1 μm thick) with 1 mm separation between two adjacent ones.[46,47,57] We

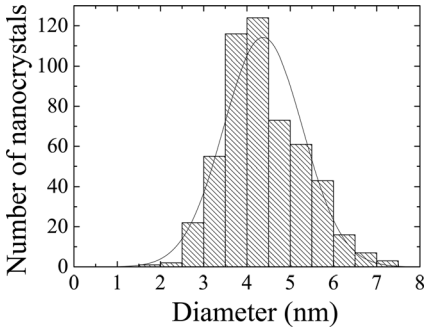

FIG. 2. A histogram of the size distribution of the Si NCs in an x ≈ 18 vol. % sample as determined from our HRTEM micrographs. The solid curve represents a Gaussian fit to the distribution. Reprinted with permission from M. Dovrat, Y. Goshen, I. Popov, J. Jedrzejewski, I. Balberg, and A. Sáar, Phys. Status Solidi C 2, 3440 (2005). Copyright © 2005, Wiley.

have carried out then standard four probe conductivity, $\sigma(x,T)$, and photoconductivity, $\sigma_{ph}(x,T)$,[46,47] current voltage (I-V) and current-time (I-t) measurements. The electrodes separation enabled us quite an accurate mapping of the dependence of the above mentioned properties on x, with a resolution of $\Delta x \approx 2$ vol. %.[46] Thus, it was possible to compare, with a good enough resolution, the $\sigma(x)$ and $\sigma_{ph}(x)$ profiles with the theoretical predictions of percolation and hopping theories. For the Si-substrated films, we have used evaporated aluminum (0.2 μm thick) or Hg point contacts where the areas of these contacts were of the order of 10^{-3} cm^2. The other electrode there was the Si wafer-substrate itself as in a metal oxide semiconductor (MOS) configuration. The main utilization of the latter configuration[47,51] was its application for the measurements of the capacitance-voltage (C-V) characteristics that were used to (indirectly) extract additional information on the transport mechanism. This was important in particular in the low-x regime where the samples resistances were too high to be measured in the co-planar[46] and even in the sandwich (vertical) configuration.[51] In our work,[47] the C-V measurements were carried out by utilizing a small ac test signal of 1 MHz and a dc bias between −30 and +30 V with a typical scan rate of 0.5 V/s. From these measurements,[47,51] we derived the concentration of the trapped charges per cm^2, N_{FB} (= Q_{FB}/q) where Q_{FB} is the stored charge (SC) per cm^2 and q is the (positive) elementary charge. The analysis used for the derivation of Q_{FB} is simple in principle[5,9,47] if the sample is assumed to represent an MOS configuration. In particular, the saturation capacitance under accumulation (positive bias at the surface contact in our samples) is assumed to be the MOS oxide capacitance, C_{ox}. A hysteresis in the bias scan is obtained by first increasing the voltage from the $V \leq 0$ to the $V > 0$ direction, until the above saturation is reached, and then, decreasing it in the opposite direction. This yields that the stored charge in the composite is approximated by $Q_{FB} = -C_{ox}\Delta V_{FB}$ where ΔV_{FB} is the width of the C-V hysteresis.

To further provide support for the models that will be suggested later on the basis of macroscopic measurements, we studied the local current routes in the samples by applying our conductive AFM (C-AFM) technique[58] to the quartz substrated samples in the dark and under illumination.[57] This measurement enables to record the current between a conducting tip (that makes contact to the sample's surface) and a side electrode. This is important in studies such as the present one, since it indicates whether the current takes place via the crystallites or in the matrix that surrounds them. This rather new type of information for ensembles of Si NCs enables then to evaluate whether a suggested transport mechanism is consistent with the observed current paths.[58] We note that this precaution of carrying out simultaneously such microscopic and macroscopic transport measurements has not been made before on ensembles of Si NCs thus leaving always some uncertainty regarding the suggested transport mechanisms.

The other, rather standard, transport measurements on our samples were of the I-V and I-t characteristics as a function of temperature. This was done by applying a voltage to the sample and determining the current by measuring the voltage drop across a small series resistor. All our transport measurements were carried out in the room temperature-liquid nitrogen temperature range by utilizing a cryostat with a temperature controller. For the measurement of the photoconductivity, we illuminated the area between two adjacent electrodes with a He-Ne laser (633 nm with a flux of 70 mW/cm^2, Refs. 46 and 47) or with a solid state laser (473 nm with a flux of 250 mW/cm^2, Ref. 57) illuminations. The difference between the current under illumination and in the dark was taken to be the photocurrent through the sample from which the value of the photoconductivity σ_{ph} was derived. In particular, noting the very informative nature of the light intensity exponent of the photocurrent γ_e (= $d[\ln(\sigma_{ph})]/d[\ln(G)]$, where G is the charge carriers generation rate that is determined by the flux of the impinging illumination[59,60]), we have also derived this quantity. In our studies, this was done for laser illumination flux over the range of 2-70 mW/cm^2.

As pointed out in Sec. I, the optical properties of Si-NCs are much better understood than their transport counterparts. As such, these properties provide a common ground for sample characterization and comparison of the Si-NCs systems.[53,56] Accordingly, our standard characterization tool of the samples was the x-dependence of their spectral photoluminescence (PL) characteristics as described in great detail[46,47,55,56] and reviewed previously.[53] Correspondingly, those will not be reviewed here beyond their complementary application in the evaluation of the transport data. We just mention then that the PL was measured under the 488 nm excitation from air cooled or water-cooled Argon lasers. The typical irradiation flux was of the order of 10 W/cm^2. In the first laser set up,[46,47] the detection was done with an optical fiber that led the luminescence signal directly to the spectrometer (Control Development Inc.), while in the other setup the PL signal was dispersed by a 1/4-m spectrometer onto a photomultiplier that fed a photoncounting system.[55,56] A confirmation of the quantum confinement effect beyond the PL data (which in principle may result from defects) was given recently by our optical transmission and ellipsometry results.[49]

III. RESULTS AND ANALYSIS

Before turning to the detailed analysis of the transport data, let us establish that we are dealing here indeed with a

system of quantum dots. In semiconductor nanoparticles, the manifestation of the size dependent quantum effects follows the quantum confinement effect as described by Eq. (1). According to the simplest theories,[2,25] this effect is expected to take place in Si NCs for crystallites with a diameter d that is less than about 8 nm. That the systems that we studied for the relatively low NCs contents fulfill that requirement is exhibited by the HRTEM image of Fig. 3, where almost equal-size spherical NCs of $d \approx 4$ nm are shown. Considering the $d \approx 2(x\text{-}8)^{1/3}$ relation that we found by the HRTEM studies,[53] we expect from the quantum confinement consideration[2,25] that the energy of the band gap will decrease with the increase of x. The standard tool for the confirmation of the quantum confinement effect is the red shift of the PL with the increase of d (Refs. 1, 2 and 54). As seen in Fig. 4, we have such a clear red shift in our samples. To eliminate any doubt regarding the possibility that this red shift is associated with states that are not connected with the quantum confinement effect,[2,53] we have turned to other optical measurements. As seen in Fig. 5, the optical transmission, $E_{G(t)}$, and ellipsometery, $E_{G(e)}$, results show a red shift of the absorption edge[49] that is consistent with the Stokes shift behavior of the PL as shown in this figure and in Fig. 4. This, of course, strongly suggests the quantum confinement scenario. However, the ultimate proof for the fact that the quantum confinement is an intrinsic effect of the NCs comes from the red shift of the bulk silicon optical transitions E_1 and E_2.[49] This is since these shifts show that the entire internal electronic structure of the NCs in our composites is changing with the NCs size. Hence, our referral throughout this review to the NCs in the systems that we studied as quantum dots is well justified.

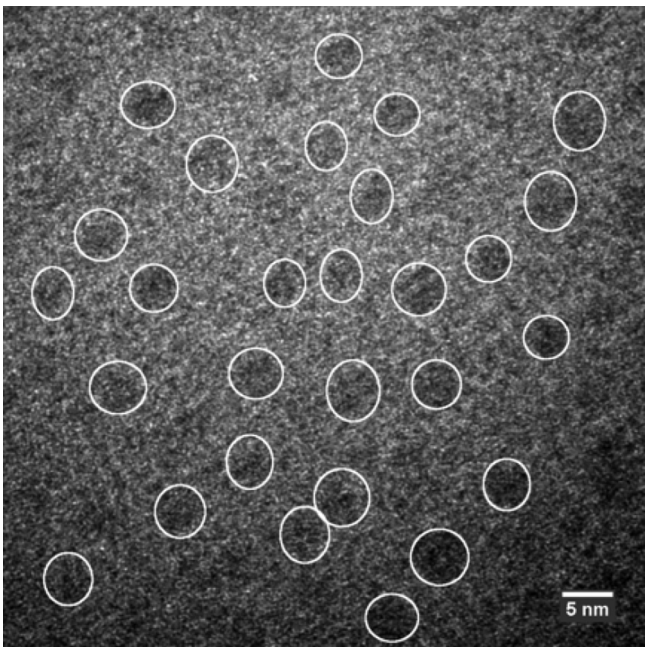

FIG. 3. A HRTEM micrograph of our annealed co-sputtered film with a Si phase content of 17 vol. %. All the NCs here are spherical and geometrically isolated from each other. Reprinted with permission from I. V. Antonova, M. Gulyaev, E. Savir, J. Jedrzejewski, and I. Balberg, Phys. Rev. B 77, 125318 (2008). Copyright © 2008, American Physical Society.

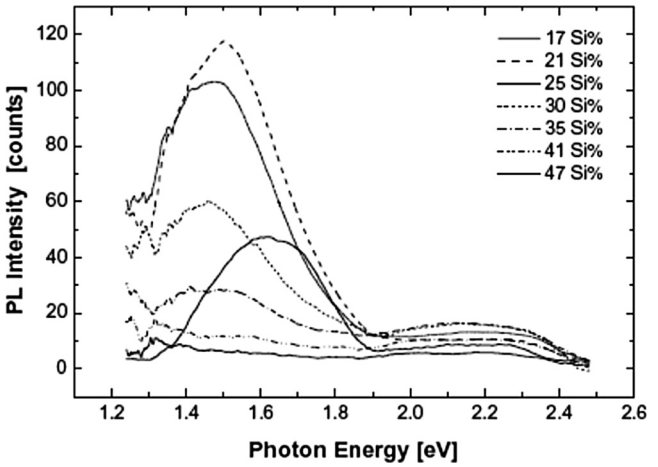

FIG. 4. The PL spectra of our co-sputtered Si/SiO2 samples for various Si contents. Note, the red shift of the PL peaks as the content x increases. Reprinted with permission from I. Balberg, E. Savir, and J. Jedrzewski, J. Non-Cryst. Solids 338–340, 102 (2004). Copyright © 2004, Elsevier.

In view of the importance that we attribute to the density of the QDs in the system as a guide for the evaluation of the transport mechanisms, we provide first an overview of the x dependencies of the most significant properties that were measured in our studies.[46,47,62] In Fig. 6, we show the typical x dependencies of the conductivity, $\sigma(x)$, the stored charge, $N_{FB}(x)$, and the PL peak intensity (at the photon energy in which this peak is observed) throughout the entire x regime. Considering the $\sigma(x)$ dependence, we note that up to about $x = 38$ vol. %, the results simply reflect the background conductance of the experimental system and thus, we cannot draw any direct conclusion regarding the transport mechanism in the $x < 38$ vol. % regime. On the other hand in the $38 < x < 60$ vol. % regime, we see a strong rise in the conductivity, and for $x > 60$ vol. %, we see a saturation (with a slight decrease) of $\sigma(x)$. We have found that this dependence can be fitted to the predictions of percolation theory[63–65]

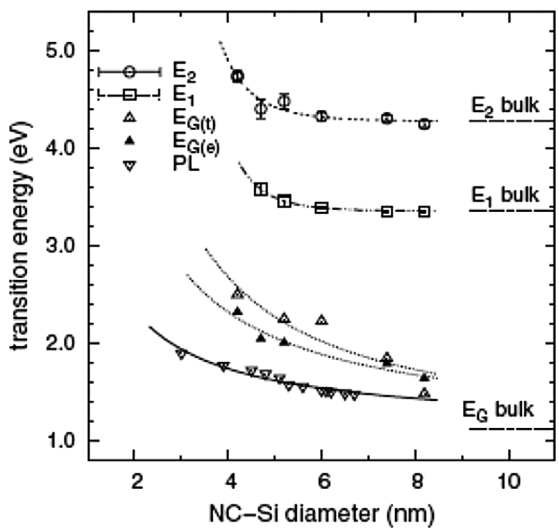

FIG. 5. A summary of our PL, optical transmission, and spectroscopic ellipsometry results. The horizontal dashed lines indicate the transitions energies in bulk silicon crystals. Reprinted with permission from M. I. Alonso, I. C. Marcus, M. Garriga, A. R. Goñi, J. Jedrzejewski, and I. Balberg, Phys. Rev. B 82, 045302 (2010). Copyright © 2010, American Physical Society.

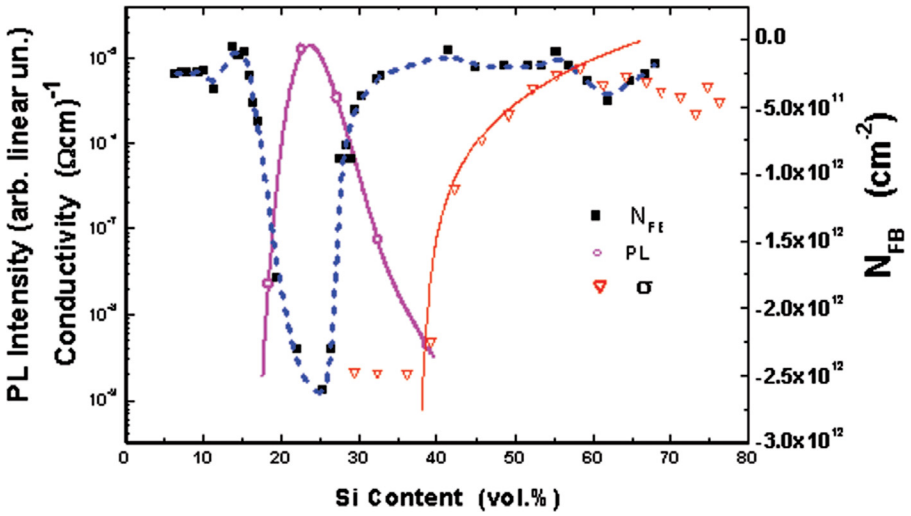

FIG. 6. (Color online) The dependencies of the stored negative charge, N_{FB} (in units of elementary charges per cm^2), the PL spectral peak intensity, and the dark conductivity, σ, on the Si phase content, x, for the entire x range of a typical sample. Comparison of these results with the predictions of percolation theory indicates that the percolation threshold is at $x_c = 36$ vol. % and that the N_{FB} and PL peaks are associated with the maximum of the concentration of the non-touching (geometrically isolated) NCs. Reprinted with permission from I. V. Antonova, M. Gulyaev, E. Savir, J. Jedrzejewski, and I. Balberg, Phys. Rev. B 77, 125318 (2008). Copyright © 2008, American Physical Society.

$$\sigma \propto (x - x_c)^t, \tag{4}$$

where x_c is the percolation threshold and t is a constant that for simple 3D systems in the continuum[63–65] has the universal-dimensional value of $t_0 \approx 2$. The dependence given by Eq. (4) is known to reflect the connectivity of the system.[63,64] We found that within our deposition and post-deposition treatments of very many samples, the typical values of x_c were in the $25 < x < 50$ vol. % range and the t values were usually in the $2 < t < 3$ range, but values up to $t = 5$ have also been observed. Following Eq. (4), we will use then the corresponding *x_c value as a prime reference point for x* in the discussion to be given below. We also found previously[46,61] that both $\sigma(x)$ and $\sigma_{ph}(x)$ have the same dependence on x. Since the number of charge carriers contributing to each of these is different, their common x dependence represents well their common connectivity-dependent mobility. As seen in Fig. 6, in contrast with the conductivity, the stored charge and the PL are significant only in the $x < 40$ vol. % regime and they exhibit their maxima (N_{FB} is negative) at the same x. We denote the value of x at the common maxima x_d and we call the x vicinity of x_d the local deconfinement regime. In Sec. III C, we interpret the common maxima to be associated with the concentration of the "geometrically isolated" NCs that have the optical features and charge retaining properties of QDs.[47] In what follows we will examine the basic characteristics of the macroscopic results of Fig. 6 by correlating them with the results of our comprehensive (mainly HRTEM) structural study. This will be done in order to consider the expectations regarding the transport in the three conductivity-distinguishable regimes ($0 < x < 38$ vol. %, $38 < x < 60$ vol. %, and $x > 60$ vol. %) that are shown in Fig. 6.

Turning now to the structural information that will guide us in the evaluation of the transport data, we show in Fig. 7, the structure that is typical for the 18 vol. % $< x < x_c$ regime. In this HRTEM image, we see some geometrically isolated NCs (that may have a small distortion from sphericity), the presence of "touching" NCs pairs and their further distortion from sphericity in regions of relatively high densities (so as to accommodate the crystallites that are grown in their proximity). For a more precise and visual definition of the concept of "touching", let us consider in Fig. 7, the NCs 1 and 2 as "touching" while we refer to NC 3 as a "geometrically isolated" or a "non touching" NC. We define then two NCs as "touching" if the distance between their surfaces does not exceed the order of a lattice constant (≈ 0.5 nm in Si). In passing, we note that the crystallographic lattice-planes in the images of the Si NCs are not parallel in the different

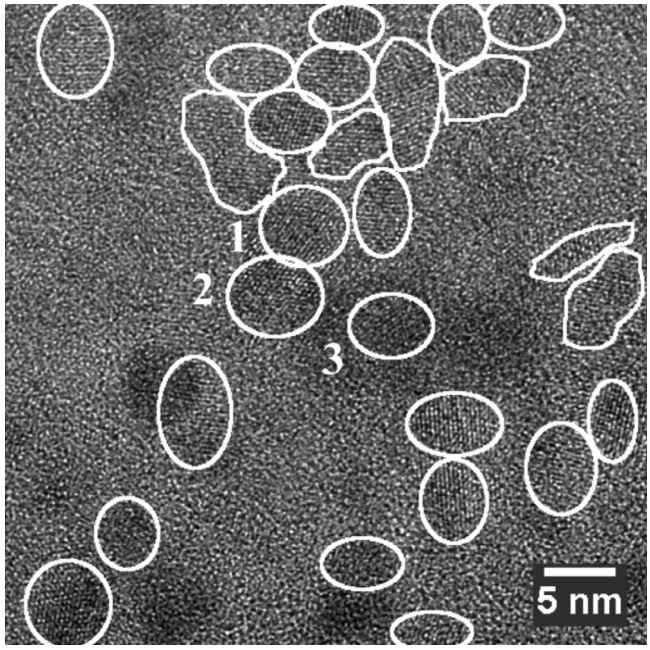

FIG. 7. A HRTEM micrograph of a sample of our annealed co-sputtered films with a Si phase content of 25 vol. %. The crystallites, identified by their Si lattice fringes, are marked by their borders. One notes that with the increase in their density, the crystallites grow and change from a spherical shape to shapes that can accommodate their density. The two NCs, 1 and 2, are defined as "touching" while NC 3 is defined as a geometrically isolated NC. Note that the increase of x causes "more and more" NCs to "touch" their neighbors. Reprinted with permission from I. Balberg, Y. Dover, R. Naides, J. P. Conde, and V. Chu, Phys. Rev. B 69, 035203 (2004). Copyright © 2004, American Physical Society.

crystallites, suggesting the independent nucleation of the crystallites during the annealing process.

Following the introduction of the "touching" concept, the results below will be presented according to a finer and more physical-processes dependent division of the above defined three x regimes. We start with the low-x regime, for which there are no "touching" NCs but the indirect data that we have, enable us to suggest the transport mechanism. We turn then to the very high-x ($>x_c$) regime that (as mentioned in Sec. I) has hardly been discussed before our recent work.[66] Our extensive and detailed transport data and analyses in this regime enable us also to analyze the experimental data in other x-regimes in terms of the "touching" concept. In particular, we will show that having a better understanding of these two extreme regimes can shed light on the x-dependent transport mechanisms throughout the so far unstudied intermediate-x-regimes.

A. The local confinement ($x \to 0$) regime

As we saw in Fig. 3, the very low-x ($0 < x < 18$ vol. %) regime consists of well dispersed (geometrically isolated) spherical NCs. These structural data indicate a geometry that is expected to yield simple intercrystallite hopping conduction, i.e., tunneling between adjacent particles. Since the SiO_2 matrix is practically insulating, this is the only inter-NCs transport mechanism possible in the low-x regime. If there is a difference between the energies of two particles, transport can take place only if this energy is supplied thermally or electrically.[8,64] In its gross features, the latter hopping conductance resembles the transport mechanism in granular metals[7,8,48] in the so-called dielectric regime. However, while in the granular metals, the energy distribution is attributed primarily to the variation in the local charging energies associated with the size and/or the environment of the individual particles, in the case of semiconductor, NCs the distribution in the particles' energy can also be attributed to discrete (localized or extended) energy levels in the network. In particular, in semiconductor NCs, the distribution of the electronic "conducting" levels is expected to be of the order of the electrostatic charging energy, as manifested by the effects of the resonant tunneling mechanism.[10,21,40]

Noting that (unlike the situation in granular metals and ensembles of Ge NCs embedded in SiO_2) we could not measure the conductivity in this, low-x, high resistance regime, we looked for other experimental approaches that can shed light on the conduction mechanism. We concluded that the combination of the images shown in Figs. 3 and 7 with the x dependence of the SC and the PL may be helpful for this purpose. The x-dependencies of the PL intensity (at its spectral peak[46,55,56]) and the SC,[47,51] as shown in Fig. 6, clearly reveal an excellent correlation between the negative SC and the PL intensity. Combining these results with structural images, such as shown in Figs. 3 and 7,[54] we conclude that there is a monotonic N(x) dependence and thus for the present $x < 18$ vol. % regime, we associate the increase of the PL and the CS with the increase in the concentration of geometrically isolated ("non touching") NCs as follows.[47] We have concluded above the presence of quantum confinement within the isolated NCs in the regime under discussion.[53–56] In fact, the optical band-gap widening that was observed in our samples[49,55,56] was shown to be of the order expected from recent theoretical estimations of the corresponding band shifts (0.1-0.3 eV).[26] Turning to the SC effect as shown by the $N_{FB}(x)$ dependence in Fig. 6, we note that the size of the NCs in our samples suggests CB energies of the order of 0.1 eV, as estimated by others[20] for Si NCs and for granular metals[8] for particles of similar sizes. While we cannot derive direct conclusions regarding the transport mechanism from the above findings, the PL and SC results suggest that both quantum confinement induced resonant tunneling and Coulomb blockade effects[10,27] control the transport. Hence, at least qualitatively, the physical nature of the inter NCs transport in the low-x regime must consist of resonant tunneling under CB. As will be further discussed in Sec. IV, it seems that our indirect evidence supports the basic Simanek-like[40] "resonant" hopping transport mechanism. This mechanism was suggested for systems such as ours in view of direct (but in the "vertical" or "sandwich" configuration) conductivity measurements in Refs. 21 and 22. In that mechanism, the ensemble of particles yield a distribution of quantized band edges as well as Coulomb blockade energies so that a hopping-like conduction between them dominates the transport.

B. The above-percolation regime

Turning to the structure of the high-x ($x > x_c$) regime, we see in the HRTEM image of Fig. 8 that in this regime, there is a further growth of the individual NCs, further distortion of the crystallites and, most importantly, the apparent presence of very large clusters of "touching" NCs. On the other hand, our C-AFM image that is given in that figure shows that the currents measured are associated with charge flow through the NCs. This is important since it indicates that our macroscopically monitored currents (that were measured on the same samples) pass through the NCs and not via possible bypassing paths (such as a possible residual a-Si network that may still be present in the sample).[57] Following these findings, we illustrate by a dark (blue) track in Fig. 8 an expected percolation current paths. One notes of course that the system is three dimensional and so the path shown indicates the existence of a global 3D percolation conductance via "touching" NCs. As will be further discussed in Sec. III E, a percolation critical exponent (see Eq. (4)) of $t \approx 2$ values that we found in general (see Sec. II) suggests that the Si NCs actually touch, rather than that the conduction between them takes place by tunneling or hopping. Such a behavior is found also in granular metals when a global network of coalescing particles is formed.[48,65–67] The possible conduction via isolated (non-touching) NCs as indicated by the bright (yellow) segments in the HRTEM image of Fig. 8 will also be discussed in Sec. III E.

The structure we observe in Fig. 8 is reminiscent of the nano-structures that were observed in three other systems, for which, unlike the present system, the transport has been studied by us and by others extensively and with which we will compare our results. Those are granular metals,[8,65,67]

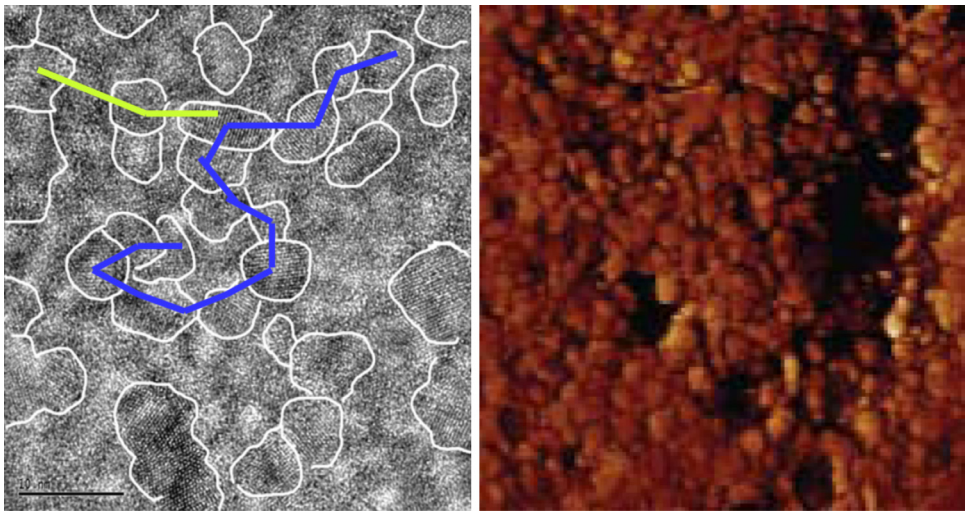

FIG. 8. (Color online) A C-AFM image of a Si phase content of 65 vol. % (right) and a HRTEM micrograph of a Si phase content of 80 vol. % (left) both of annealed co-sputtered films. The C-AFM image (1 μm $\times$ 1 μm and current range 0-4 pA under the application of 5 V) shows that the current takes place via the crystallites while in the HRTEM micrograph (40 nm $\times$ 40 nm), a continuous network of "touching" NCs is seen to be formed. A typical continuous current path is illustrated by the dark (blue) segments on the micrograph. A possible tunneling current path via a DBTJ-like configuration is marked by the light (yellow) segments in the micrograph. Reprinted with permission from I. Balberg, Y. Dover, R. Naides, J. P. Conde, and V. Chu, Phys. Rev. B 69, 035203 (2004). Copyright © 2004, American Physical Society.

hydrogenated microcrystalline silicon (μc-Si:H),[58,68] and semi-insulating polycrystalline silicon (SIPOS).[37,69–71] Starting with granular metals, the common features of interest are that above the percolation threshold, x_c, a continuous network of conducting particles is formed, and that the particles can be charged with energies that are larger than the room temperature kT. The major differences are that (unlike the granular metals) the carrier concentration in semiconducting particles is variable, "touching" particles do not coalesce geometrically or chemically,[72] the charging is associated with specific (bulk or surface) states[9] and the discreteness of the internal levels may play a role in the transport for temperatures that are not extremely low (<1 K).[21,27] The second system of interest is that of μc-Si:H when the crystallites are in the $d < 10$ nm range.[38,73] In this system, in the high crystalline regime (but below the formation of crystalline columns) a percolation network of touching Si crystallites may also form.[58] On the other hand, that system differs from ours by the fact that there is Hydrogen there and thus the surrounding matrix is of hydrogenated amorphous silicon, a-Si:H, rather than SiO_2 as in the present system. We may expect then that a different electronic states distribution within the NCs, but that not too different boundaries between touching NCs will form in the two systems. Considering the above differences, the closest system to that of ours seems to be the SIPOS, but again, this is only when the crystallites are in the $d < 10$ nm range.[37,71] We note though that, unlike in the system studied here, in SIPOS, as is the case in μc-Si:H, hydrogen may still play a major role.

Having the above background, let us turn now to the results obtained from our transport measurements. We already noted above that in the high-x regime, we have the ability to carry out a direct study of the transport. Here, the conductivity is large enough to enable one to follow the changes as a function of external parameters, the most common of which are the temperature and the applied voltage. In what follows, our presentation of the corresponding dependencies that we measured will be accompanied by a critical discussion of the difficulties associated with the possible interpretations. We will show that our comparative study of these dependencies, and other dependencies in various systems that we intentionally prepared, enabled us[66] to narrow down substantially the number of possible transport scenarios in the present regime of $x > x_c$.

Let us begin then by showing in Fig. 9, typical σ(T) and σ_{ph}(T) dependencies that we obtained for a co-sputtered sample of $x \approx 67$ vol. % (where for the corresponding entire co-sputtered film x_c was 31 vol. %). The temperature range in all our measurements was $80 < T < 300$ K. We start, in Fig. 9(a), with the most common presentation of such data i.e., as a log σ vs 1000/T dependence. Trying to fit these results by an Arrhenius plot

$$\sigma = \sigma_A \exp[-(T_A/T)], \tag{5}$$

where σ_A and T_A are constants of the system, we see that the data cannot be fitted by a straight line, i.e., for the temperature range that we studied, it cannot be accounted for by a single activation energy value, E_a (= kT_A). On the other hand, we could fit the data with two activation energies E_{a1} and E_{a2} (solid curve) by assuming that $\sigma = \sigma_1 + \sigma_2$, where σ_1 is the asymptote to the σ(T) data at the low temperature end and σ_2 is the asymptote to the σ(T) data at the high temperature end. The excellent fit obtained suggests that we have either two processes activated in parallel or that we have a process that is composed of a series of excitations with activation energies distributed between the above two E_a values. This behavior (as will be discussed in detail below) is very typical of many homogeneous (ordered[9] or disordered[74–76]) semiconductors, where the carrier excitation is determined by more than one source (e.g., two different donor energies or a continuous distribution of electronic states) or by changes in the mobility activation energy.[9,77]. In principle, the origin of the donating, or transport conducting levels, may be even associated with quantum confinement.[78] We should point out already here that the combination of the E_a

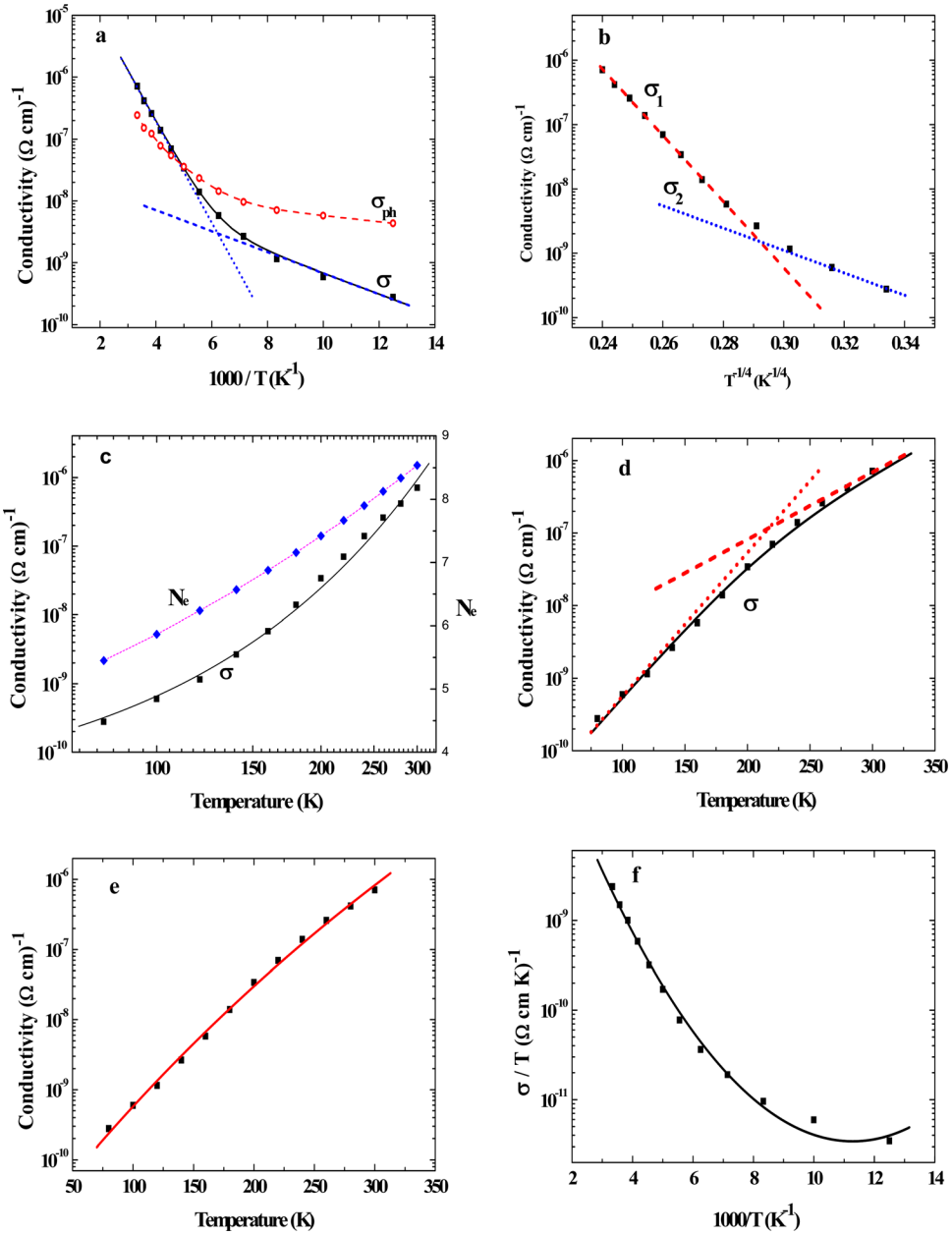

FIG. 9. (Color online) The temperature dependencies of the dark conductivity σ (and the photoconductivity σ_{ph} (a)), as measured at V = 40 V, in the high-x ($\approx 67 > x_c = 31$ vol. %) regime. The same dark conductivity data are fitted by various dependencies that were suggested according to corresponding transport mechanisms in the literature. (a) A single Arrhenius plot cannot fit the entire data but the same data (σ) can be well fitted by a parallel addition ($\sigma_1 + \sigma_2$) of two such plots. (b) A single "Mott $T^{-1/4}$" dependence cannot account for the entire data but, again, two such plots can account for them. (c) The concave behavior of the σ(T) data can be hardly fitted by a single Berthelot dependence. Assuming that the data can be fitted to a $\sigma \propto T^{\delta}$ dependence with a temperature dependent $\delta = N_e\text{-}2/(N_e + 1)$ yields the N_e values that are shown in this figure. (d) The σ(T) data can be well fitted by a series combination (i.e., $\sigma^{-1} = \sigma_1^{-1} + \sigma_2^{-1}$) of two Berthelot dependencies. The data are very well accounted for by the "$T_1/(T + T_2)$ " dependence, (e), and by the "a-b/$T + c/T^2$" dependence, (f). Reprinted with permission from I. Balberg, Y. Dover, R. Naides, J. P. Conde, and V. Chu, Phys. Rev. B 69, 035203 (2004). Copyright © 2004, American Physical Society.

value at the high-temperature end and the structural data will be our main tool in the evaluation of the most likely transport mechanism in the present regime. Returning to Fig. 9(a), we also see that throughout the entire temperature range, the σ_{ph}(T) dependence exhibits a milder variation with temperature than σ(T). Hence, if corresponding activation energies are deduced, the ones for σ_{ph} are smaller than those of the corresponding dark conductivity. This behavior is typical of semiconductors, in general[59] and in disordered Si systems in particular,[79] and is usually explained by the shift of the demarcation level (at which the trapping rate equals the recombination rate) towards the Fermi level, E_F, with increasing temperature.[59] This σ_{ph}(T) behavior may support the possible presence of a continuous distribution in energy of trapping-recombination centers between the conduction band edge, E_c, and E_F. Since the qualitative behavior of the many samples that we measured was the same i.e., in all of them, we found a non-single activation energy and a milder variation of the photoconductivity, we will not present more of the measured dependencies here. On the other hand, in our more detailed analysis, we will stress the self consistent interpretation of these features and the correlation between the quantities that we derived from them (such as $\sigma(T = 300\ K)$ and $E_a(T = 300\ K)$ or $\sigma_{ph}(T = 300\ K)$ and γ_e(T)) and the structural data shown in Fig. 8. However, before doing that, let us evaluate the data shown in Fig. 9(a) in light of some transport mechanism theories that were, or may be, suggested for the interpretation of such data.

Following the "popularity" of the interparticle hopping model (see Sec. I), we tried to fit our above σ(T) data to a dependence of the form

$$\sigma = \sigma_H \exp[-(T_H/T)^{\gamma}], \tag{6}$$

where, $\sigma_{H,}$ T_H, and γ are constants of the system. Again as with the trial to fit the data to Eq. (5), we could not find any

single T_H value, for any $1/4 < \gamma < 1$, to fit the entire data to Eq. (6). On the other hand, as shown in Fig. 9(b), the σ(T) data can yield a good fit to a $\sigma = \sigma_1 + \sigma_2$ dependence with the same or different T_H and/or γ values in the high and low T regimes. One must note, however, that as was pointed out by many authors before[80] (but still ignored by many others), over the temperature range studied here (and of course when only part of it is utilized[81]), it is essentially impossible to distinguish reliably between fits with different γ values (in the $1/4 \leq \gamma \leq 1$ range). Correspondingly, the derivation of a γ value from data such as ours (with no other supporting evidence) cannot prove the presence of a hopping conduction mechanism. Hence, a behavior with $\gamma = 1/2$ (or $\gamma = 1/4$) (that was attributed by some authors[22,81] to a hopping-like conduction between the NCs) without support by other evidence cannot be considered conclusive. In particular, one notes that the T_H values by themselves (that some authors compared with theoretical predictions) do not provide a reliable criterion. This is since in disordered semiconductors, one is concerned in general with energies of the order of 1 eV and with typical densities of crystallites and/or defects of the order of 10^{17}-10^{19} cm^{-3}. Thus, the agreement of the value of T_H with the order of magnitude of the density of states (DOS) values does not really tell us much as to the nature of the transport or its corresponding network. It appears then that the suggestions that were based solely on the σ(T) data[15] for single x values do not stand up to the criterion of an additional support for the hopping-like models. As an example, we can consider a recent suggestion of hopping in a system of Si NCs (Ref. 23) where the density of the NCs has not been specified. Hence, it is not clear whether the $\gamma = 1/2$ value, that was determined there, is claimed for the hopping regime that was mentioned in Sec. III A or is it claimed for the high-x regime of concern here. As discussed in Sec. IV, while the first possibility may be appropriate, the second possibility is in contradiction with the analysis to be presented below, that relies on the σ(x,T) dependencies.

The σ(T) dependencies that we discussed (Eqs. (5) and (6)) describe a convex log σ vs. log T behavior. Since we could not fit, our data with single T_A, T_H, and γ values, we turned to fit the data by a concave dependence. Indeed, as shown in Fig. 9(c), presenting the same data in the log σ vs log T scales shows such a concave dependence. In view of that, we turned to fit the data to a single Berthelot-dependence,[82–87] $\sigma = \sigma_B \exp[(T/T_B)]$, that is known to represent a concave log σ vs. log T behavior. Here, σ_B and T_B are the fitted parameters of the dependence. While this type of dependence is known in other fields,[82] it is much less abundant and much less understood in solid state physics. Still, it has been found in some semiconductor[83,84] and some nano-semiconductor[85–87] systems and was suggested to be associated with thermally activated tunneling via a barrier. In some cases,[83,85,86] it has been attributed to an activated barrier-vibration process, while in others,[84,87] to a barrier which has an energy peaked profile. In the latter models, the resultant observed Berthelot-like behavior was suggested to be determined by the resultant effect of the needed thermal excitation energy and the width of the barrier; the higher the temperature, the larger the number of carriers that can tunnel through the narrower part of the barrier, such that the maximum tunneling probability yields the Berthelot-like behavior. While, as shown in Fig. 9(c), the Berthelot fit does not yield an accurate behavior it may be considered "reasonable". However, if one assumes a series connection of two resistors with two different T_B values, one obtains, as seen in Fig. 9(d), an excellent fit to a $\sigma^{-1} = \sigma_1^{-1} + \sigma_2^{-1}$ dependence. Indeed, the later fit was suggested by Fisher *et al.*[88] for the barrier fluctuation model but for a very different system. The σ_1 and σ_2 that they used were the Berthelot asymptotes at the high and low ranges of temperature. The same physics, i.e., the increase of the tunneling probability that follows the effective lowering of the barrier height due to thermal fluctuations, was suggested also by other models.[88,89] Utilizing here the corresponding dependence of Sheng *et al.*,[89] $\sigma \propto \exp[-T_1/(T+T_2)]$, where T_1 and T_2 are system parameters, we could fit well our σ(T) data. In fact, as shown in Fig. 9(e), we could fit the data there by a single set of T_1 and T_2 values. While seeming successful, one should note that this good fitting is associated with quite a "flexible" exponential function (since it has an extra parameter in comparison with the Berthelot function) and as such, it can also be well fitted to dependencies found in ordered or disordered homogeneous systems where the suggested fluctuating-barrier theory is not applicable at all. A somewhat different barrier type model was suggested by Werner.[90] That model is based on the assumption that there is a given fixed-in-time Gaussian distribution of the barrier heights such that $\sigma/T \propto \exp(a - b/T + c/T^2)$ where, a, b, and c are constants. In Fig. 9(f), we see that with this kind of fit the "parabolic contribution" to the "left branch" of the parabola enables a "flexibility" that brings about a relatively good fit to the data. We must note then, again, that the "good" fit to the experimental dependence with a relatively large number of parameters, in comparison with the above simpler dependencies, does not necessarily indicate the applicability of the suggested mechanism. As all the above dependencies for systems that are reminiscent of ours were suggested in the context of potential barriers in general, and between semiconductor crystallites in particular, the experimental approach that we applied in our works was to test the σ(T) and I-V behaviors in systems where there are no barriers or, where the barriers, if they exist, are very different from those of the systems mentioned above.

Returning briefly to the abundant non barrier model, i.e., the hopping model, let us consider in some more detail, the σ(T) behavior exhibited in Fig. 9(c). This behavior can be attributed, in principle, to a variable range hopping (VRH) like process.[91,92] In this VRH the hopping range decreases and thus the number of hops in the transport path increases, with increasing temperature. The prediction of the corresponding hopping model is that $\sigma = \sigma_0 T^{\delta}$, where $\delta = N_e - 2/(N_e + 1)$ and N_e is the number of hops in the transport path. The physical picture of this model is that the conduction process is associated with a 1D-like network conduction rather than with a 3D-like conduction network. Trying to fit our data to this σ(T) prediction, we determined the slope δ (from Fig. 9(c)) and derived from it the "expected number" of hops according to the above $\delta(N_e)$ relation. As seen in this figure,

N_e changes between 5 and 9 over the studied temperature interval. We note, however, that in studies[92,93] on rather homogeneous systems that are much smaller than our 1 mm contact separation, the typical N_e values were also in the $1 \leq N_e \leq 12$ range. This suggests, again, that a good fit of the data to a given $\sigma(T)$ dependence cannot make, a priory, the corresponding mechanism more plausible than any of the other mechanisms that were described above.

Considering the fact that $\sigma(T)$ results, such as ours, have been found in all the disordered Si systems that were mentioned in Sec. I, we can state that one cannot judge a priori which of the above fittings is the "best". One should consider then the data within a context that can eliminate at least some of the mechanisms that we mentioned above. We further note that one can in principle improve ones conclusions (but, again, as described below, only to a limited degree) by considering the I-V dependencies that are suggested for the corresponding mechanisms.

Let us examine now whether the I-V dependencies can provide by themselves more unique conclusions than the $\sigma(T)$ dependencies. To do that we show, in Fig. 10, a typical I-V characteristic of a typical sample ($x \approx 50$ vol. %) on log I vs V (a) and log I vs log V (b) scales. We see clearly that the same data show excellent fit to both, an $I \propto \sinh \kappa V$ dependence (where κ is a constant) that corresponds to one of the barrier models,[88] while the other plot suggests a change of the logarithmic slope from 1.12 to 1.85 that corresponds to a transition to a space charge limited current[9,14,59] behavior. In fact, this also applies to a Fowler-Nordheim tunneling dependence[9] but a priori we rule out this mechanism here since the applied voltage in the system that we study is dropping along very many intercrystallite barriers and thus, we expect to get (as in tunneling characteristics for low applied bias) a linear I-V dependence. Correspondingly, we further note that quite in general, the linearity of an I-V characteristic may conceal the actual mechanism that the theories predict for a single barrier or junction. Thus, we must conclude here too that trials to evaluate the conduction mechanism solely on the basis of such I-V fits have the same drawbacks that we encountered in the attempts to draw conclusions solely on the basis of the experimental $\sigma(T)$ data.

The above discussion is expected to convince one that even the combination of both, the $\sigma(T)$ and the I-V dependencies, cannot yield a unique determination of the transport mechanism. Correspondingly, it became apparent to us that additional evidence is needed in order to determine more conclusively the transport mechanism in the high-x regime. As most of the above interpretations are associated with transport through potential barriers, we turned to examine experimentally the corresponding mechanisms more thoroughly by preparing pairs of samples such that in some of them, the presence of barriers is unlikely and others in which potential barriers are expected to exist. We have compared then the $\sigma(T)$ and I-V dependences in such pairs of samples. In fact, in order to overcome the uncertainties in the interpretations of the results, a rather comprehensive study of these dependencies as a function of x was required.[66] The sample pairs that we prepared were co-sputtered in parallel and after the sputtering, electrodes were deposited and conductivity measurements were taken on one film of a pair (i.e., the non annealed one). The other film was subjected to the annealing procedure (1200 °C, 50 min) described in Sec. II, and only then electrodes were provided and the sample was measured. Indeed, our Raman (see Fig. 1) and IR spectroscopies confirmed that the non-annealed samples contained a mixture of a-Si and SiO_2 phases, while following annealing, we had samples of Si NCs that are embedded in the SiO_2 matrix (see Figs. 3, 7, and 8). In addition, we sputtered also Si-only films (with no co-sputtering of SiO_2) that definitely have a different structure than that of the co-sputtered Si/SiO_2 films.

A general observation on the many samples that we have examined (sputtered, co-sputtered, doped, and undoped) was that for the non-annealed samples, the I-V characteristics were linear for any value of x. This, as shown in Fig. 11, is in sharp contrast with the annealed samples where the I-Vs became non-linear when the percolation threshold was approached.[46] We note of course that these findings are consistent with a continuous a-Si network in the non annealed samples and with the existence of DBTJs in the vicinity of x_c, in the annealed ones.[46] Turning to the $\sigma(T)$ measurements, we found that qualitatively the dependence in all the samples studied was the same, i.e., as in Fig. 9(a). To characterize the behavior of the $\sigma(T)$ dependence, we considered mainly the room temperature value of $\sigma(300\ K)$ and the activation energy at room temperature, E_a. We found first[66] that for the sputtered Si-only films, the annealing did not change considerably the value of E_a, even though the conductivity has changed by about two orders of magnitude. In contrast, in the co-sputtered films (i.e., the Si/SiO_2 composite), we found that for the non-annealed samples,

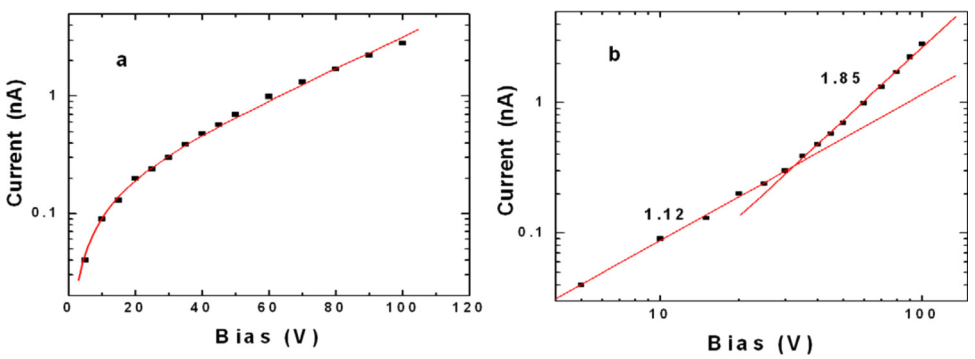

FIG. 10. (Color online) Typical room temperature I-V characteristic for a sample of $x = 50$ vol. % (where $x_c = 31$ vol. %). The data are fitted by the $I \propto \sinh \kappa V$ dependence, (a) and by two segments of a power-law dependence with the exponents given in the figure, (b). Reprinted with permission from I. Balberg, Y. Dover, R. Naides, J. P. Conde, and V. Chu, Phys. Rev. B 69, 035203 (2004). Copyright©2004, American Physical Society.

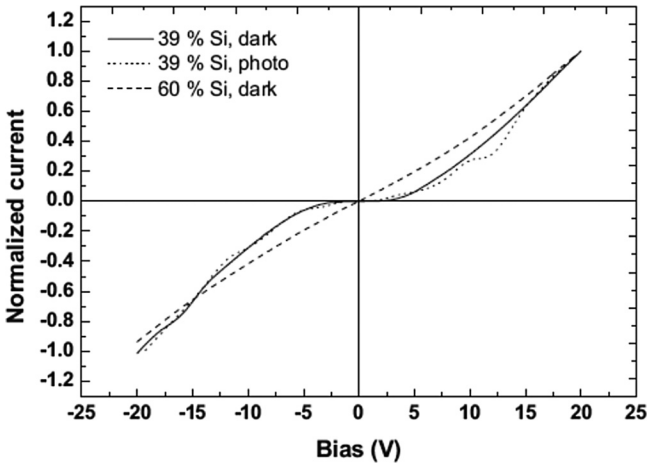

FIG. 11. Normalized (at 20 V) current-voltage characteristic in a sample with a Si content of 60 vol. % (dashed curve) and the current- and photocurrent-voltage characteristics in a sample with a Si content of 39 vol. %. Note the much more emphasized non-linearity for the sample with the lower silicon content. Reprinted with permission from I. Balberg, E. Savir, J. Jedrzejewski, A. G. Nassiopoulou, and S. Gardelis, Phys. Rev. B 75, 235329 (2007). Copyright © 2007, American Physical Society.

E_a was nearly constant for the $x > x_c$ range and it increased slightly as the percolation threshold was approached, while for the annealed samples, E_a increased considerably upon this approach (e.g., from 0.17 eV, for $x/x_c = 1.59$ to 0.26 eV, for $x/x_c = 1.15$). We further noted in our survey of the sample pairs that the variation of the E_a values with x in a given film was larger than the variation of the E_a values between the annealed and non-annealed samples. Combining these observations with the behavior of the above mentioned I-V characteristics, we concluded that the properties of the Si/SiO_2 systems are quite different from those of the a-Si-only systems and that the difference is strongly manifested by the increase of E_a upon the approach to x_c in the Si/SiO_2 system. To establish the above conclusions even more convincingly, we carried out also a comprehensive study of our doped samples (where in the co-sputtering process, the Si source was an n-type Si wafer with a resistivity of 0.005 Ω cm that is expected to have a concentration of 10^{18} cm^{-3} donors,[94] see Sec. II). That study was carried out because the higher conductivity of the doped films enabled us to approach more closely the vicinity of x_c. For these films, for example, we found that in the non-annealed samples E_a increased from 0.095 eV (at $x/x_c = 1.65$) to 0.14 eV (at $x/x_c = 1.23$) while for the annealed samples *E_a increased from E_a = 0.10 eV (at x/x_c = 1.65) to 0.35 eV (at x/x_c = 1.05)*. These results suggest that in the high-x ($x > x_c$) regime, the two systems (annealed and non-annealed) are similar when the x value is removed from x_c but they differ considerably when x approaches x_c. Combining the above results for x well above x_c, with the corresponding general observation of linear I-Vs for both the non-annealed and annealed samples, it appears that all these systems, for $x \gg x_c$, are very similar as far as the origin of the E_a value is concerned. Considering the many results on the role of oxygen doping in crystalline Si,[95] a-Si:H,[96] μc-Si:H,[97] and SIPOS (Refs. 69 and 71) systems, and the apparent present lowering of E_a that accompanies the increase of the conductivity upon phosphorus doping, we concluded that E_a reflects the carriers activation energy in all these systems.[66] In particular, we noted that the oxygen donors in silicon are located 0.16-0.17 eV below the conduction band edge,[71] very close to the E_a values that we found for the undoped $x \gg x_c$ samples. It turns out then that our study of the doped samples clearly indicates the similarity between the system that we studied here and SIPOS. In addition, for the n-type samples with wafer-targets of resistivities of 20-30 Ω cm ($N_D \approx 10^{15}$ cm^{-3}), 0.15 Ω cm ($N_D \approx 10^{17}$ cm^{-3}), and 0.005 Ω cm ($N_D \approx 10^{18}$ cm^{-3}), we found that while in the non-annealed samples, the conductivities were independent of the doping, for the annealed samples, the results were dependent on the doping. For example, at $x/x_c = 1.30$, the observed conductivities were 10^{-6}, 10^{-5}, and 10^{-3} $(\Omega\ cm)^{-1}$ respectively. This is quite an important observation in the present context since our values are very close to those observed in SIPOS samples[69] that were annealed under similar conditions to those used in our studies. Thus, we see that the system studied here is very similar to the SIPOS system and that the effect of hydrogen (that is present in the SIPOS but absent in our samples) is not too significant in the two systems. In passing, we remark that for our p-type samples, we derived similar conclusions.

Following the above described observations, let us reconsider now some of the possible mechanisms that we mentioned in the context of Fig. (9), that were suggested for disordered solids, in general,[88,98] for SIPOS (Refs. 69, 71 and 99) and for μc-Si:H (Refs. 38, 68 and 100) systems. We will argue first which of these mechanisms are not likely, or at least not well supported, for the systems studied here and then we will try to suggest a self-consistent picture of the conductions mechanism in the presently considered $x \gg x_c$ regime. As many of the models proposed for the explanation of the dependencies of the types presented in Fig. 9, in general, and for SIPOS and μc-Si:H, in particular, were concerned with the presence of potential barriers between the crystallites, we turn to the evaluation of these models in view of our observations. In some of the studies on SIPOS and μc-Si:H systems, the $\sigma(T)$ results were interpreted by various thermionic emission models that are, in principle, consistent with our findings of an increase of the "activation energy" with temperature (a concave log σ vs log T behavior). However, the fact that in our study, the activation energies are quite similar for systems where barriers may exist (as in the annealed, co-sputtered, samples, Figs. 7 and 8) and in samples, consisting of a continuous a-Si network where barriers are not expected to exist (the non-annealed samples), suggests that the E_a values are not associated with a barrier effect. We note also that barrier models such as that of Kapoor *et al.*,[87] while being very appealing (due to their simple rigorous derivation), assume a particular barrier-shape (in order to obtain the Berthelot behavior), but they do not explain how such a barrier comes about. Moreover, it is hard to imagine that the same barrier shape will be obtained for our annealed and non-annealed samples and/or with and without the SiO_2 phase. The situation is much the same with the I-V data. The linear I-Vs that we obtained in our samples for $x \gg x_c$ indicate that, at least for that regime, the non-linear I-Vs obtained in barrier controlled systems[69,88] are not relevant to the presently studied system. In addition, the corresponding barrier models and the hopping models[91,92]

cannot explain the presently observed non-linear I-V behavior as x_c is approached.

Considering the above doubts as to the applicability of the simple barrier and hopping (non-Arrhenius) models to the systems that are the subject of this review, we are left with the interpretation of the $\sigma(T)$ dependence as reflecting a variable activation energy. Such a variation can come about either from the shift of E_F through a given distribution of states,[99] as is common in disordered semiconductors,[77] or from the variation of the dominant thermionic emission channel when a barrier between two crystallites exists.[37,69,71] Since both types of interpretation have been proposed for SIPOS (Refs. 71 and 99) and since SIPOS-like systems resemble most closely the NCs/SiO_2 composites that we discuss here, we consider both of them below. We shell argue that in the systems of Si NCs that we studied the two models amount to the same. We point out however, that the E_F-shift picture is conceptually a more justified one as it is consistent with the fundamentals of transport in disordered semiconductors.[101]

Turning to the model of thermionic emission, we start by noting that while hinted about previously,[100] the following consideration has not been included explicitly in the discussions of common semiconductor barrier models, such as that of Seto.[37,69–71] This is that for crystallite sizes ($d < 10$ nm) that we have in the present work and that Seto[37] had in his samples, there is no meaningful space charge region-induced surface barrier but rather a simple uniform semiconductor. In the latter case, as suggested by Baccarani *et al.*,[70] E_a is simply equal to E_c-E_t, where E_t is the energy of the surface states. This conclusion follows from the request of charge neutrality, i.e., from the fact that the density of the charge trapped in the surface states N_t' will adjust itself to become $N_t' = N_D d$ where N_D is the concentration of the donor states in the bulk of the crystallites and N_t ($> N_t'$) is the maximum available surface states density. For small enough crystallites then, if $N_D d < N_t$, there will be no barrier at the surface but a readjustment of the Fermi level in the sample. Once this is the case, the entire ensemble of crystallites forms a bulk-like system that consists of a continuous network of crystallites with a single, well-defined E_F that is a priori determined by the combined state distribution of the crystallite interior and its surface. Considering the small size of the crystallites in the systems that we studied the necessary $N_D d > N_t$ condition for the formation of a space charge region is not fulfilled. This is simple to see from the fact that in the annealed samples, the doping is effective and the value of N_D (by intentional and non intentional doping) is not larger than 10^{18} cm^{-3}. Hence, for the $d \leq 10$ nm range considered in our samples, we have that $N_D d \leq 10^{12}$ cm^{-2}, but this is well known to be the lower limit estimate of N_t in SIPOS.[37] Hence with no formation of barriers, we must assume that we have a "continuous" network of crystallites with a common E_F that is determined by the various electronic states in the system. An additional support to the applicability of such a "network" model to the nanocrystallites system that we studied is the agreement of our $\sigma(N_D)$ results with those of Seto's for N_D in the 10^{15}-10^{18} cm^{-3} range. This shows that the system that we studied is indeed very similar to the SIPOS systems in the $N_t \geq N_D d$ regime. Moreover, we note that for the crystallites sizes and densities involved in our samples, the concentration of donors (say, of the order of 10^{18} cm^{-3}) amounts to a single electron per crystallite, so that the concept of a double Schottky-like (semiconductor-semiconductor) space charge barrier becomes invalid. Following the above analysis, we suggest[66] that one cannot describe the conduction mechanism in a system such as ours by thermionic emission but rather as transport in a network of a disordered semiconductor. The important point is then that in the case of small enough crystallites, there is no way to distinguish between the model of a single carrier excited in a semiconductor, where E_F is determined by the DOS distribution in the bulk, and the Seto,[37] or the other more detailed models of thermionic emission.[69,70] Therefore, we conclude that the condition $N_t = N_D d$ marks the transition between a behavior of a barrier model and a behavior of the E_F shift within the corresponding landscape of the states distribution.[101] It appears to us, in passing, that the present conclusion was overlooked in the past works since the interest in those studies was in the variation of N_D, while in the present work, the interest is in the quantum confinement regime[47,56] and thus, the emphasis is on the crystallites size d. Considering now the resemblance of the present system to SIPOS, we note that the concave $\sigma(T)$ behavior in the latter system was interpreted by Hamasaki *et al.* already in 1977 (Ref. 99) in terms of the E_F shift with temperature, in the band tail landscape of states. However, this was done without specifying the role of the oxygen dopant (as we suggested previously for μc-Si:H (Ref. 68)) and/or the surface-bulk relation that we mentioned above. Following Hamasaki *et al.*, the model that we suggest here is based on a continuous states distribution in the "mobility gap" and not on the presence of semiconductor barriers. Again, we emphasize that the distinction between the two models can be meaningful only for large enough crystallites, while for the crystallites of the sizes involved in this work (i.e., where $N_t > N_D d$), the models are undistinguishable.

The picture of thermal excitation from band tail states (having a continuous distribution in their energies) to the conduction band that we just presented is further supported in our case by the photoconductivity data of Fig. 9(a). This is since the corresponding dependence is similar to that observed in many works on μc-Si:H.[68,79] Hence, the $\sigma_{ph}(T)$ dependence can be simply interpreted as due to the temperature induced shift of the demarcation level within the band tail-like states in the macroscopic system.[59] Our comprehensive study of μc-Si:H (Ref. 68) has shown that dependencies such as $\sigma_{ph}(T)$ in Fig. 9(a) and $\gamma_e(T)$ in Fig. 12 are conclusively associated with band tails, and that these tails are very different from those that we found in a-Si:H.[60] Following our structural data (Fig. 8) and the fact that after the sample annealing, we do not have a-Si in our Si/SiO_2 samples (see Fig. 1), we conclude that (as in μc-Si:H (Ref. 68) the inter-crystallite boundaries yield the "surface" states of the NCs and that the latter have a band tail-like distribution. In fact the simplest interpretation of the $\gamma_e(T)$ dependence follows the relation $\gamma_e(T) = T_0/(T_0 + T)$, where kT_0 is the width of the band tail.[59] Correspondingly, the $\sigma(T)$ dependence suggests that (similarly to E_F) the quasi-Fermi level, E_{Fq}, shifts

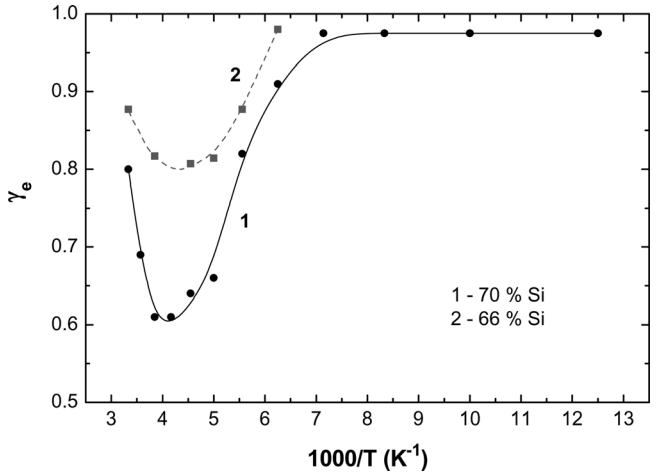

FIG. 12. Typical temperature dependence of the light intensity exponent, γ_e, for samples of x = 70 and x = 66 vol. %. The curves shown are the best fits to the data. The structure of the samples on which these data were obtained is similar to the one shown in Fig. 8. These results are very similar to those obtained for μc-Si:H. Reprinted with permission from I. Balberg, Y. Dover, R. Naides, J. P. Conde, and V. Chu, Phys. Rev. B 69, 035203 (2004). Copyright © 2004, American Physical Society.

down with increasing T so that at low T, it scans the "steeper" part of the band tail (that is close to the mobility edge E_c) while at higher temperatures, it scans the deeper-wider tail part of the band tail.[99] Hence, the initial decrease of γ_e(T), expected from the above relation, is followed by an increase with increasing T. This is in agreement with the fact that in all disordered silicon systems, from a-Si:H to polycrystalline silicon, the band tails always widen towards the center of the midgap.[102] Another possible mechanism that may be applicable for the interpretation of the γ_e(T) dependence is the one[103] that considers the role of the mobility with increasing temperature. According to that model if the mobility is temperature activated, the spatial range of states involved in the recombination with the increase of T may yield an effective increase in the separation between the two demarcation levels. This opposes the regular temperature-induced "statistical" decrease of the demarcation levels' separation.[59] Other, more detailed models involve the role of the two band tails and the recombination in both of them.[68,104] For our analysis, however, the important consequence of all those models is the common feature of a continuous distribution of states in the pseudo gap and the presence of a temperature promoted competition between two contradicting effects. These, in turn, are in agreement with the two conclusions that we suggested above, i.e., the dominance of the band tail state distribution and the down shift of E_F with increasing temperature. Hence, these conclusions further justify our view that the system behaves as a continuous disordered semiconductor. We suggest then that the increase of γ_e with decreasing x, as indicated in Fig. 12, follows the increased recombination rate as the network become sparse due to the increase in the concentration of the total NCs surface area and thus the density of the "surface" states. Our suggestion is supported by the fact that the γ_e values increase with the decrease of the illumination wave length (from 628 nm to 437 nm) as expected from the enhanced light absorption at the surface and thus enhanced surface recombination.[9] A significant observation regarding the photoconductivity is that with increasing doping, we get an enhancement of σ_{ph} which is also consistent with the band tail model since the quasi Fermi level is closer then to E_c, i.e., the doping shifts the E_{Fq} (just as it does for E_F) upward in a landscape of the band tail.[105]

One interesting conclusion that we can also derive from the discussion given above is that for small size crystallites, the crystallite and its surface are a single electronic unit, so that a potential barrier, in the usual sense, does not form and we have a network of crystallites that acts as a homogeneous continuous entity. Our present conclusion is consistent with the much broader physical picture of the Si-NCs/SiO_2 system that we studied. This is since there is structural evidence for an oxide shell that wraps the crystallite[106] and since there is spectral-optical (mainly PL) evidence for the idea of a one-electronic entity that consists of a small crystallite with an oxidized surface.[107] Our own interpretation of the strong PL intensity in the presently studied system[26,53,55] does also rely on the strong electronic coupling between the surface and the bulk of the NCs. It appears then that, in general, the system of Si NCs embedded in the SiO_2 matrix is a network of bulk-Si/surface-SiO_2 nanoparticles, such that at the low-x regime, this provides the strong PL, and at the high-x regime, it constitutes a continuous network. In all the electrical and optical effects, the role of the surface is to be expected since the surface constitutes a large portion of the NC.[53] For example, if we assume that the thickness of the SiO_2-like surface of the Si QD is of the order of $\eta = 0.5$ nm and the diameter of the Si core of the crystallite is of the order of $a = 6$ nm (as in the high x-regime), the surface shell to bulk volume ratio becomes larger than ($6\eta/a$ =) 0.5, which is considerably larger than in the planar geometry (η/a) for which the barrier models have been suggested. Hence, the role of the crystallite's surface is very significant in the determination of the electrical and optical properties of the presently studied system of Si NCs.

In view of the above results and our detailed analysis, we are able now to suggest the following comprehensive interpretation of our results in the high-x regime. The annealed and non-annealed samples have continuous state distributions that determine the position of E_F with respect to the band edges. For x far enough above x_c, if E_F is pinned by (say) unintentional donor states, the carriers activation energy, E_a is just E_c-E_F. The fact that doping does not change the value of E_a in the non-annealed samples suggests that E_F is indeed pinned in those samples as is the case of a-Si.[77] In contrast, in the annealed samples, the density of states in the "mobility gap" is considerably smaller, enabling E_F to upshift with doping and thus to approach E_c, lowering the value of E_a. In particular, we found a variation of E_a with doping in the doped-annealed samples and conductivity values as those found in SIPOS (Refs. 37 and 69) for the same concentration of phosphorous donors. Also, we note that the oxygen donor in various Si systems is located around $E_D = E_c$-0.16 eV,[71] in excellent agreement with the interpretation given here for the results found in the annealed undoped Si-SiO_2 system. We suggest then, in the spirit of Hamasaki *et al.*,[99] that the σ(T) behavior is simply a

reflection of the E_F shift within the "landscape" of a continuous distribution of states[101] that are present in the crystallites. Those states are due to disorder and doping (mainly oxygen donors and acceptors). Our model accounts also for the relatively low conductivity in the network of the touching NCs compared to that of crystalline Si bulk. The low conductivity can be understood then by viewing the interface regions between the crystallites (see Figs. 7 and 8) as a source of carrier scattering. The corresponding model, as suggested previously by Tarng[69] for polycrystalline Si, considers the quantum mechanical reflection and the relatively low tunneling transmission through these interfaces, even in the case of rather narrow "mismatch" barriers (between touching NCs) such as those that we see in Fig. 7. Turning to the strong increases of E_a and the enhanced non-linearity in the I-Vs, as x approaches x_c from above, we suggest (as detailed in Sec. III E) that the increase of E_a is simply due to the additional charging-quantum confinement energies in that regime. The transport is not controlled then by the barriers between "touching" crystallites, but rather by the barriers associated with the oxide regions (wider than 1 nm) that become significant when the NCs dispersion becomes sparse. The corresponding tunneling transport via these barriers is illustrated by the light (yellow) segments in the HRTEM image of Fig. 8. This explanation is consistent with that of He *et al.*[38] for μc-Si:H (with Si NCs smaller than 10 nm). The very important conclusion that we derive then for the regimes where the HRTEM images show touching between NCs is that the physical consequences of the touching are as those between coalescing particles in granular metals.[72] The interfaces between the touching NCs act as carrier scatterers that do not involve surmountable tunneling barriers. We note also that this interpretation of the transport is also in accord with our explanation of the PL quenching when two crystallites "touch", i.e., that the latter pair acts as a single electronic entity with a diameter that is larger than the exciton-Bohr diameter of Si (8.6 nm).[47]

Finally, we did not discuss the low temperature $\sigma(T)$ behavior because in the high-x range, the $\sigma(T)$ dependence "flattens" and no unique reliable $\sigma(T)$ dependence can be deduced. This result can be due to a measurement artifact (e.g., one may measure a "parasitic" part of the circuit or a leakage resistance) or it may represent a genuine low-temperature conduction mechanism such as tunneling or hopping. As we saw already in the discussion of Fig. 9(b), in the limited temperature range of our study, the attempts to fit the log σ data to a $T^{-\gamma}$ behavior are not amenable. Hence, we have considered in this review only the E_a values derived at room temperature. At this point, it is not clear however whether the low temperature $\sigma(T)$ dependence reflects a temperature induced shift of E_F through states[101] (as we suggested above for the conveniently measurable higher temperature range), a hopping mechanism between some (as yet unspecified) states, or an experimental limitation.

C. The local deconfinement regime

Following the understanding that we acquired for the extreme NC density regimes, we can conveniently analyze now the transport in the intermediate-x regimes. In Fig. 6, we followed the increase of the SC and the PL with increasing x and this (as discussed in Sec. III A) was well accounted for by the increase in the concentration of the NCs in the low-x regime. A further increase in x yields, however, a decrease of the SC and the PL. As a result, a peak in their x-dependence is observed at some Si phase content x_d which for the case shown in Fig. 6, is around $x = 24$ vol. %. On the other hand, as seen from the HRTEM image of Fig. 7, it is apparent that while, with increasing x, there is a continuous increase in the total concentration of the NCs, N, the latter increase is accompanied by a decrease in the concentration of the non touching NCs, N_1. Correspondingly, we explain the decrease in both, the SC and the PL intensity for $x > 24$ vol. %, as due to the decrease of N_1 with increasing x.[47] Considering the PL, we note that the exciton Bohr diameter in Si is 8.6 nm (Ref. 34) while the diameters of the NCs in our samples for this x regime is of the order of 5 nm (Refs. 54 and 55). Following our conclusion that the network of "touching" NCs acts as a continuous semiconductor, we expect that the clusters of "touching" NCs will act as single, large, particles. Even clusters of two NCs will have an effective diameter that is at least in one direction, larger than the above exciton's Bohr-diameter. Correspondingly, these NCs will not contribute to the PL, due to the deconfinement of the electron-hole pairs. Hence, in practice, out of the total concentration of the NCs, N, the only NCs that contribute to the PL are the N_1 "geometrically isolated" (or non touching) ones. This interpretation of the PL dependence on x is strongly supported by predictions from percolation theory.[63] In that theory, above a certain particle concentration N_d, the increase of the average cluster size with N will be associated with a decrease in the concentration of the geometrically isolated particles.[47,61] This will result in a peak in the $N_1(N)$ dependence that will be manifested in our case by a peak in the PL intensity. In particular, percolation theory[63] predicts that the peak of the $N_1(N)$ dependence will be found at $N_d \equiv 2N_c/3$, where N_c is the critical concentration of all the NCs at the percolation threshold. Considering the $N \propto x$ relation, this suggests that $x_d \approx 2x_c/3$. Indeed, as seen in Fig. 6, we found that for a typical sample with $x_c = 36$ vol. %, the peaks of the PL and the SC are at $x \approx 24$ vol. %.[66] This excellent agreement with the prediction on the cluster statistics in percolation theory[61] can only be interpreted as suggesting that only the non-touching (or "geometrically isolated") NCs contribute to the PL and CS. Thus, we associate the latter observation with the deconfinement of the electron-hole pairs. Hereafter, then, we refer to the above common peak of the PL and SC as the "local deconfinement peak". Similarly, we attribute the x dependence of the SC to the increase and then to the decrease of the charges associated with the isolated NCs.[47,61] In other words, the larger clusters play the role of electrical shorts in the system and this facilitates the discharging of the sample.

Following the above and our considerations in Sec. III A, we conclude now that the dominant conduction in the $x \approx x_d$ regime is expected to be tunneling between the various entities in the system i.e., the small clusters and the non-touching NCs. While the hopping conduction will still be controlled by

the isolated NCs, the clusters, with their smaller confinement and Coulomb blockade energies, will play an increasing role as x increases. It is not impossible that this is the explanation for the VRH ($\gamma = 1/4$) behaviors that were reported in some works on ensembles of Si NCs.[52,81,108] However, the lack of even an approximate value for x in those works does not enable to confirm this possibility at present. In turn, this underlines our emphasis on the importance of the density (N or x) of the NCs. On the other hand, while we concluded above that the cluster statistics has a profound effect on the SC and the PL, we do not expect a priori a significant change in the sample conductance, in comparison with the low-x regime, since the "bottle necks" for transport, for the $x \approx x_d$ regime, will still be the tunneling effect between the non-touching NCs. Correspondingly, it is not impossible that with the increase of x, one will observe a transition from the Simanek behavior[40] to a VRH behavior.[81] Experimentally, however, a distinction between the two behaviors will need a considerable refinement of the current measurement techniques.

D. The intermediate, $x_d < x < x_c$, regime

A priori, one would expect that the $x_d < x < x_c$ regime will simply exhibit an enhancement of the features that were suggested in the previous regime (Sec. III C). This is since, as seen from Figs. 3 and 7, the main effect of the increase of x is the increase of N and the formation of clusters at the expense of the "non-touching" individual NCs. However, the increase of x beyond the $x \approx x_d$ regime yields larger and larger clusters so that the distance between them decreases. Following the coalescence-like behavior between touching NCs, we may consider now the narrowing of the junctions between the various clusters with increasing x, thus yielding a higher tunneling conductivity between them. We expect that the VRH-like transport, in the low-x end of the regime, will give way to tunneling between "large" (multi-NCs) clusters at the high-x end of this regime. This scenario is very much like the situation that was encountered previously in granular metals,[48] except that here the conduction mechanism associated with the "touching" NCs is as in disordered semiconductors rather than in a disordered metal.[72] We note though that the presently discussed regime has not been studied and/or discussed in detail even for the relatively simple systems of granular metals. On the other hand, while we do not know of explicit studies of ensembles of semiconductor NCs in this regime, the expected higher conductivity here, in comparison with that of the $x \approx x_d$ regime, suggests that it may be studied soon. In fact, such studies may be motivated by the expectation that the present and previous NCs density regimes are crucial for optoelectronic applications (such as electroluminescence). This is since achieving, simultaneously, efficient transport and efficient PL are the two ingredients needed for the development of these applications.

Similarly, as in granular metals,[48] we expect that the competition between the intra-cluster conduction (as in Sec. III B) and inter-cluster tunneling[109] (as in Sec. III C) is sensitive to the structure that is imposed by sample preparation and annealing conditions. This suggestion is supported theoretically by the type and size of clusters that can form under different fabrication conditions[110] and, experimentally, by the non-monotonic σ dependence on the metallic content in the intermediate metallic content regime of granular metals.[48] However, the lack of direct information regarding the $\sigma(x)$ and the $\sigma(T)$ dependencies in the regime under discussion does not allow us to follow the variation of the transport mechanism there as a function of x. Correspondingly, we can only base our anticipations on the results of Fig. 6 and the above considerations. We expect that in the presently discussed intermediate-x regime, the transport is dominated by a mixture of mechanisms that varies from a Simanek-like inter-NCs hopping[40] to some inter-cluster tunneling[48] as x increases.

E. The percolation threshold regime

In this $x \approx x_c$ regime, the non negligible conductance enabled us to study the transport directly. In fact, we were able to show[46] that the $\sigma(x)$ dependence in Fig. 6 is in excellent agreement with the predictions of the critical behavior of percolation theory as given by Eq. (4). However, in view of the fact that for this regime, various hopping mechanisms were suggested, we start here by analyzing the $\sigma(x)$ dependence in terms of inter-NCs hopping. Unlike the predicted percolation behavior, as given by Eq. (4), the predicted dependence that assumes only intercrystallites hopping is based on the expectation that the inter-particle tunneling route will prefer the nearest neighbors that correspond to the average lowest tunneling resistance that enables a continuous percolation path. In that hopping-like case, one can further show that

$$\sigma \propto \exp\left(-\alpha x^{-1/3}\right), \tag{7}$$

where, α is a known constant.[64,65] This dependence applies in the dilute (low-x) limit and can be easily shown[65] to become of the form $\sigma(x) \propto \exp(-\alpha' x^{-1})$ (where the constant α' replaces α) in the denser (higher-x) case. As seen in Fig. 13, the trials to fit our $\sigma(x)$ data to these dependencies failed, showing that the simple hopping scenario does not apply to our system in this regime. In contrast, we found (following our well checked fitting procedure[111]) that these results are well characterized by the percolation power law given by Eq. (4) with $x_c = 31$ vol. % and $t = 2.5$.

While the above results indicate that percolation is the most likely mechanism to account for the $\sigma(x)$ dependence in this $x \approx x_c$ regime, we note that it does not exclude the possibility that the interparticle conduction is by tunneling. Considering the latter, the exponential decay of the local tunneling conductance between two spherical particles is given by[112]

$$G = G_0 \exp(-2\chi(r - d)), \tag{8}$$

i.e., the contribution of the farther conducting-sphere neighbors to the transport will diminish exponentially with the increase of their tunneling distance r-d. Here, G_0 is a constant that accounts for the charge carrier concentration and the local particle environment around $r = 0$, and $1/\chi$ is the tunneling decay (sometimes referred to as the localization[64,65]) length of the wave function of the charge carrier. It turns out that even

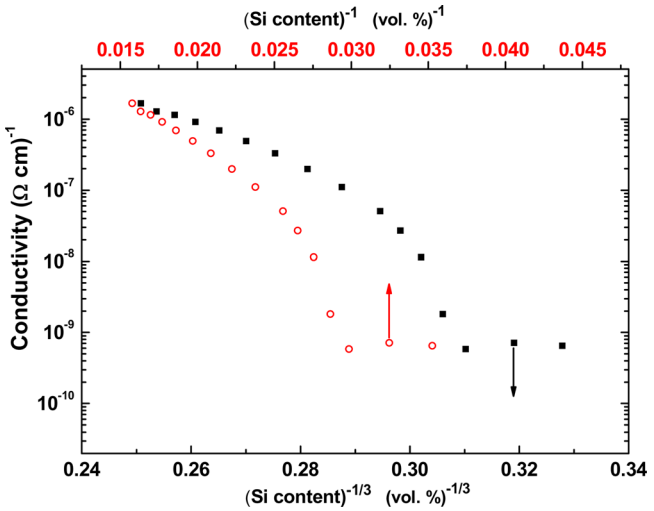

FIG. 13. (Color online) A typical $\sigma(x)$ characteristic when presented on a $x^{-1/3}$ (solid squares) and a x^{-1} (open circles) scales. The lack of linearity in these scales indicates that for the $x > x_c$ regime, the conductivity cannot be accounted for by intercrystallite hopping. On the other hand, when presented according to Eq. (4), these data reveal a percolation behavior with a percolation threshold, x_c, at 31 vol. % and a critical exponent of 2.5. Reprinted with permission from I. Balberg, Y. Dover, R. Naides, J. P. Conde, and V. Chu, Phys. Rev. B 69, 035203 (2004). Copyright © 2004, American Physical Society.

under tunneling conduction the conductivity can still yield a percolation-like behavior but the value of the exponent t appears to be non universal and its value can be approximated by $t_0 + u$, where, t_0 is the universal-dimensional value (of about 2 in 3D systems) and $u = 2\chi(a\text{-}d/2) - 1$ where 2a is some average distance between nearest neighbors.[64,67] According to the percolation-tunneling theory,[111] u can be only positive. Correspondingly, one can "theoretically" define two particles at a "surface" distance of $r_{ij} = r\text{-}d$ as "touching" when $r_{ij} < 1/(2\chi)$ and particles for which $(r_{ij}) > 1/(2\chi)$ as non-"touching." Considering the fact that usually $1/\chi$ is of the order of 1 nm (Refs. 7, 8 and 112), we may define two particles, the surfaces of which are no more than 0.5 nm apart, as touching particles. We see that the result of this definition is in excellent agreement with the empirical definition of touching that we based on the TEM image in Fig. 7, as well as with our criterion that this distance is of the order of the Si lattice constant (see the introduction to Sec. III). This justifies our use of the tunneling decay distance as our self consistent criterion for "touching" throughout this paper. We further expect then that a network of such "touching" particles will yield (as found for coalescing particles in granular metals[48,67]) a universal (i.e., $t \approx 2$) critical behavior. On the other hand, if the conduction-percolation network is determined by tunneling via larger distances (i.e., via the SiO_2 matrix), a non universal percolation behavior (t significantly larger than 2) may be expected.[65,67] Indeed, in our previous works on granular metals,[65,67] we found that there are two percolation transitions, one that takes place (in the so-called dielectric regime[8]), for non-coalescing metal grains, at 18 vol. % (Ref. 67) and one that takes place for coalescing grains[67,109] around 50 vol. % of the metallic phase. The first transition is associated with the onset of percolation-tunneling connectivity[65,67] and the other (at the higher vol. % of the metallic phase) is associated with the formation of a continuous metallic network.[8,48,109] While in the first transition, a non-universal t value of 3.3 was observed and in the second (higher metallic content) transition, the universal $t \approx 2$ value was obtained.[8,48,67] As mentioned above, the non-universality is due to the effect of the distribution of the tunneling distances between the non coalescing (non touching) grains. The fact that the t values that we found here are usually close to 2 indicates that the percolation transition in our samples is determined by a continuous network of touching NCs just as that of the coalescing metal grains. A more complete picture is obtained by noting that in the Si NCs system that we study here (at variance with the case of granular metals[8,48]), the Si NCs do not coalesce, geometrically. The latter was manifested in Figs. 3, 7, and 8 by the different orientations of the crystallographic planes in the "touching" crystallites, in spite of their close proximity. Following this and the understanding that we gained in Sec. III B, the transport in the ensembles of "touching" NCs can be considered as taking place in a "dirty semiconductor." This is in very close analogy with the concept of "dirty metal" that has been used[8] to describe the metallic network above the higher-x percolation threshold in granular metals.

Let us consider now the inter-particle charge transfer effects that may accompany the percolation process. We expect that when x is made to approach x_c from above, we will find some geometrically isolated NCs that are critical in the electrical network. Such single particle "bottlenecks" are expected[46] to show a DBTJ behavior.[10] That this is geometrically likely is illustrated by the bright (yellow) segments in Fig. 8. Also, electrically, such "non-touching" single NCs are expected to show local charging effects.[10] The fulfillment of this expectation is exhibited by the temperature dependent normalized current vs. voltage characteristics that are shown in Fig. 14. These characteristics that were taken at a bias scan rate of 0.07 V/s differ from the results of slow scans (scan rate less than 0.01 V/s and at room temperature[46]) of

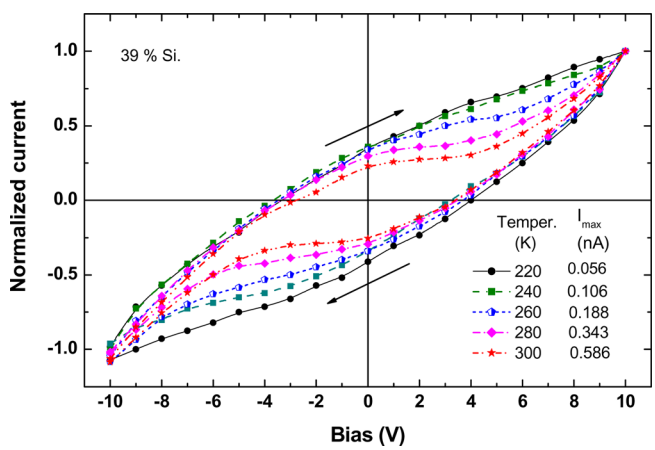

FIG. 14. (Color online) (a) The measured normalized (each by its I_{max}) I-V characteristics as obtained, under a bias scan of 0.07 V/s, for a sample in the close vicinity ($x = 39$ vol. %) of the percolation threshold (here, $x_c = 37$ vol. %). The hysteresis "shrinks" and the "voltage gap" are more pronounced as the temperature is increased. Very similar I-V characteristics were obtained for the photo-currents. Reprinted with permission from I. Balberg, Y. Dover, R. Naides, J. P. Conde, and V. Chu, Phys. Rev. B 69, 035203 (2004). Copyright © 2004, American Physical Society.

Fig. 11, by exhibiting a temperature dependent hysteresis. The "flat"-horizontal portions of the I-Vs in Fig. 14 are the "split" parts of the voltage gap that become less and less apparent as the temperature decreases, due to the corresponding larger "RC" time at the lower temperatures. We note here that, as with increasing temperature, the lowering of the scan rate (from 1 V/s to 0.02 V/s) has the same effect, i.e., the hysteresis ceases and the voltage gap split decreases, until the voltage gap segments "unite" around the ($I = 0$ and $V = 0$) origin.[46] In accordance with the findings of Fig. 11, these phenomena are apparent for x values in the close vicinity of x_c (= 37 vol. % here) but they do not appear to exist away ($x > x_c$) from this vicinity.[46] We conclude then that there is a stored charge in the conducting network that tends to discharge with time and that the discharge is accelerated with increasing temperature. Another manifestation of the charging effect is exhibited in Fig. 15, where we show the I-t characteristics in the close vicinity of the percolation threshold. As we see in the figure, both the application and the removal of the voltage are accompanied by a current decay but, upon bias termination, there is an inversion of the current sign. Again, such a behavior is typical only of the close vicinity of x_c. For $x > x_c$ (say, $x = 60$ vol. %), no such charging or discharging effects are found within the (1 s) resolution of the present measurements. In Fig. 15, we denoted the initial and the steady state currents of the process by I_0 and I_s, respectively.

In order to confirm that charging effects are responsible for the results shown in Figs. 14 and 15 and in order to quantitatively determine the stored charge, we have measured (with an applied voltage of 5 V) both a hysteretic I-V characteristic, such as in Fig. 14, and an I-t characteristic such as in Fig. 15. In our work,[66] we determined the stored charge Q from both groups of data. The simplest way for deriving the value of Q is to consider the "area" $Q = \int[I(t)-I_s]dt$ following the bias application or the "area" $Q = \int I(t)dt$ following the bias termination. The other simple approach is to consider the above I_0 and I_s values and using for the analysis,[66] the simplest equivalent circuit that captures the essence of the system i.e., the so called Wagner circuit.[113]

The analyses mentioned above and those of the hysteresis loops in Fig. 14 were found to yield Q values that were in agreement with those derived (as described in Sec. II) for the corresponding x values from our C-V data analysis for the same applied bias.[47] In particular, all of them indicated that the SC is of the order of 3 nC, which corresponds to about 5×10^{15} cm^{-3} elementary charges in the coplanar configuration of our samples. One should note, of course, that this means that at the $x \approx x_c$ regime less than 1% of the crystallites in the system are charged. This finding supports our conjecture that in practice only the single-individual, non-touching NCs, retain their charge (see Sec. III C), on the one hand, and the existence of DBTJs in this regime, on the other hand. The results that suggest the "local" nature of the charging effect are the temperature dependencies of I_0 and I_s. As shown in Fig. 16, we found, that the activation energy of the charged state (I_s) is higher than that of the initial state (I_0) indicating the same charging effect as the hysteresis in Fig. 14, i.e., the presence of a Coulomb blockade. In fact, the difference between the two activation energies is of the order expected[20] for a single DBTJ (here, 0.05 eV). This gives further support to our interpretation in Sec. III B that the increase of E_a as $x \rightarrow x_c$, is associated with the Coulomb blockade effect. Of course, we note that the 1/T range is relatively narrow here due to the high resistance of the samples in this $x \approx x_c$ regime, but this range is sufficient for the indication of the proposed CB effect.

All the above data suggest that indeed at the $x \approx x_c$ regime, the conductivity is dominated by DBTJ-like configurations that are associated with "non touching" NCs that are situated between large clusters of "touching" crystallites.[46] This also supports our tunneling interpretation of current

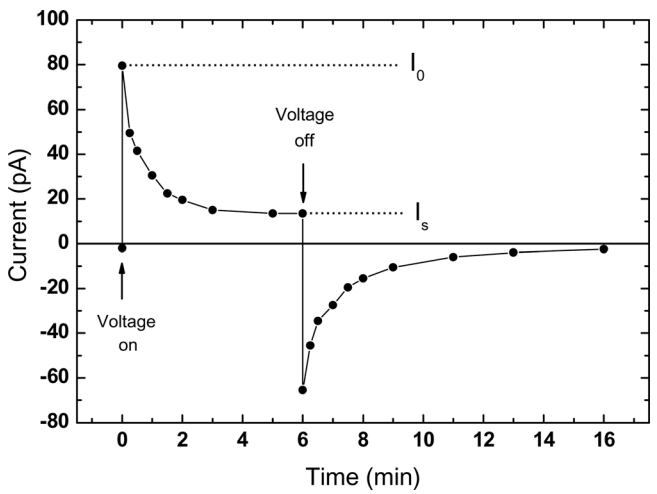

FIG. 15. A typical I-t characteristic as obtained for a sample in the very close vicinity of x_c ($x = 37.7$ vol. %,) under the application of a bias of 5 V. Note that the current decay and response to switching provide evidence for substantial charge storage. This behavior is obtained only in the close vicinity of x_c. The initial current, I_0, and the steady state current, I_s, are indicated in the figure. Reprinted with permission from I. Balberg, Y. Dover, R. Naides, J. P. Conde, and V. Chu, Phys. Rev. B 69, 035203 (2004). Copyright © 2004, American Physical Society.

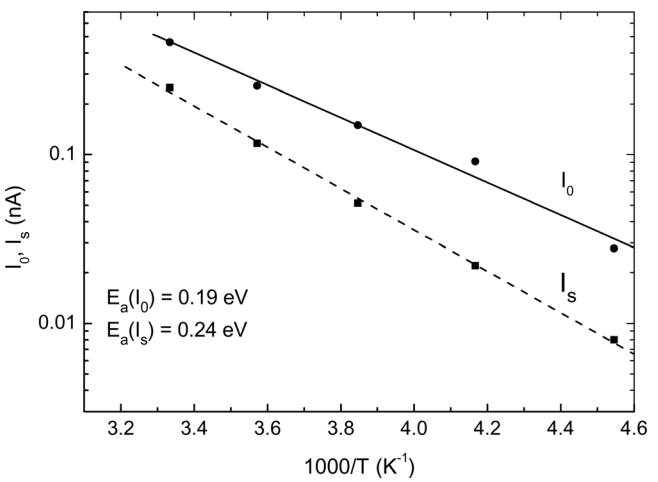

FIG. 16. The temperature dependence of the initial and steady state currents for a sample in the very close vicinity of x_c ($x = 37.7$ vol. %) under the application of a bias of 20 V. Note that there is a difference in the activation energies for the two currents. Reprinted with permission from I. Balberg, Y. Dover, R. Naides, J. P. Conde, and V. Chu, Phys. Rev. B 69, 035203 (2004). Copyright © 2004, American Physical Society.

routes in the structural image given in Fig. 8 as indicated by the light (yellow) segments in the figure. It is interesting to note in passing that the DBTJ configuration[46] that we concluded here from a macroscopic study of the system can reproduce the DBTJ characteristic in a microscopic single electron transistor that is fabricated by lithographic techniques.[15]

The above data do not disclose whether the voltage gaps that we found[46] are due to level splitting associated with the QC and/or the CB of the individual DBTJ crystallites. However, our indirect data that revealed a particularly large photovoltage[57] and our optical evidence for the quantum confinement effect suggest that both effects determine the DBTJ-like behavior. It should be pointed out that the scaling of the measured voltage gap, in terms of a DBTJ configuration, will require some specific models. We note though that this voltage is of the order reported for single NCs (Refs. 15, 19, 22 and 114) and for 2D systems where the in-plane conduction via an ensemble of the NCs has been measured.[115] This yields further support to our present interpretation of the results as due to the critical DBTJ configuration in the close vicinity of x_c.

IV. DISCUSSION

In the present review, we have presented results of electrical and optical measurements from which we tried to determine the evolvement of the transport mechanism as a function of the density of Si QDs in 3D ensembles. While the understanding of the transport in these systems is at a rudimentary level, the very basics of the electronic structure of the single Si NC is relatively well known to be that of a quantum dot. The latter topic was investigated in many theoretical[2,25,26,33] and experimental, optical absorption,[2,24,49] and PL,[2,53,56] studies. It is quite well established from those studies that the band edges shift, so that the band gap widens, by up to 0.8 eV as the NC diameter is reduced to 3 nm.[53,55] In comparison with these achievements from optical studies and the success of local transport measurements on NCs of other semiconductors,[27,32] one finds that for the Si NCs various microscopic or microscopic-like electrical measurements did not lead to a self consistent picture of the conducting levels in them. This appears to be the case in spite of the many I-V and C-V measurements on small clusters and 2D systems (in the vertical configuration) of Si-NCs.[5,15] Our assessment follows in particular from the fact that no two studies yielded the same set of energies for the single NC and from the fact that there were no microscopic electrical studies that have been checked for self consistency with simultaneous optical or other characterizing measurements. Usually, the results were compared with *ad hoc* models that were proposed to explain particular features in the experimental data.[5,15,20] From these studies, it also appears that the CB effects overshadow the QC effect in spite of the expectation[20,34] and the indirect evidence[21,57] that the energies observed are of the order of the predicted QC energies for the NCs. Correspondingly, the basis on which one can interpret the available transport data in 3D systems is still quite narrow. The approach we took as reviewed here was primarily to exclude some of the transport scenarios that were proposed for the 3D ensembles of Si QDs and then to suggest the most likely one. In particular, this review is aimed to point out that without specifying the density and the sizes of the NCs involved in the studies, the "popular" suggestions that the transport in the NCs ensembles involves hopping and/or thermionic emission mechanisms[15] are not well founded. In fact, we tried to show that the hopping is limited to the lower NC densities and that the thermionic emission is quite an inappropriate description for the small NC sizes involved in the ensembles of the Si QDs systems under discussion. We have derived the most likely transport mechanisms in ensembles of Si NCs by studying, systematically, the transport properties as a function of the NCs density. In contrast with the approach that we took in Sec. III, where we presented new information and concepts, we will discuss now the systematic evolvement of the transport mechanisms with the increase of the Si quantum dots density as given by x.

Starting with the very dilute ($x < x_d$) ensembles of Si NCs, the presence of only geometrically isolated individual spherical NCs suggests that only a hopping-like transport mechanism can take place between them. There are, however, very few direct data in the literature to justify this expectation in ensembles of Si NCs, and the more convincing evidence for that mechanism came in fact from a study of ensembles of Ge NCs embedded in a SiO_2 matrix.[21] Those data showed that the variations in the dark conductivity, σ, between the values obtained for 4 vol. % and 15 vol. % Ge resemble the variations found for similar metallic contents in granular metals such as Ni–SiO_2.[8,65,67] The absolute σ values were, however, five-to-six orders of magnitude smaller in the Ge-SiO_2 ensembles than in their granular metal counterparts. This behavior is not unexpected if we attribute the difference to the concentration of electrons available for conduction within the conducting particles in the two systems. On the other hand, if a more detailed $\sigma(x)$ dependence (such as Eq. (7)) would have been presented along the temperature dependent data, the suggested hopping conduction in the Ge-SiO_2 ensembles[21] would have been more convincing. In particular, it would have indicated that the hopping is between the NCs and not between defects in the system. Also, we note that the temperature range in that study was significantly smaller than the one applied in granular metals studies for the establishment of the $T^{-1/2}$ dependence.[8,48] The problem with a limited temperature range is exemplified by the study of Banerjee[81] on ensembles of Ge NCs embedded in a SiO_2 matrix that claimed to find that $\gamma = 1/4$. A careful analysis of his data reveals more the difficulties[80] in deriving reliable γ values, from the limited T range that was studied, than yielding the actual γ values. In fact, one can fit his data almost equally well to a linear $\log \sigma \propto \log T$ or to a $\gamma = 1/2$ behavior. This, and the fact that the measurements were carried out perpendicular to a very thin layer of Ge NCs with an unspecified density do not enable then to conclude an inter-NCs-3D VRH behavior as claimed by the author. On the other hand, even in Ref. 21, the more detailed nature of the hopping process is questionable. In particular, it is not clear between which electronic levels the tunneling takes place. In

contrast, it is clear that in that study,[21] the tunneling-controlled carrier injection from the contacts adjusted itself to the concentration of carriers in the Ge NCs as explained by the much larger conductivities than those found in ensembles of Si NCs. This suggests that intercrystallite hopping did indeed take place in that work.

Since, there are at least five theoretical models that are a priori suitable for the interpretation of the results in the low-x regime[7,8,39,40,64] and since there are only a few reliable experimental data it seems hard at the present stage to choose the exact hopping mechanism that dominates this regime. However, in view of the apparently reliable $\gamma = 1/2$ value and the "right order of magnitude" of the T_H values (see Eq. (6)) reported for Ge (Ref. 21) and Si (Ref. 22) NC ensembles, the results, as suggested by the corresponding authors, can be definitely interpreted on the basis of the Simanek model.[40] We recall that in that model, a "resonant tunneling" in the presence of a Coulomb blockade and a distribution of NC sizes and inter-NCs distances is assumed. Our work provides further (though indirect) support to that interpretation since our optical data[49,55,56] and SC data[47,66] for such dilute ensembles show the existence of QC and CB effects as well as the presence of a wide enough distribution of NC sizes.[53,54] We note of course (see Eq. (3)) that for ensembles with no such distribution of sizes, we do not expect the quantum confinement to affect the transport since $\Delta E_{QC} = 0$. This may explain why in 2D arrays of NCs with nearly equal size of the NCs systems, or in systems of a few crystallites,[5,15] the E_{CB} is well revealed while it is hard to observe the ΔE_{QC} effect. Following all the above, we assume at present that the Simanek[40] hopping mechanism, as suggested in Refs. 21 and 22, is the most likely one to represent correctly the transport mechanism in the regime of the low density ensembles.

The new important ingredient in the discussion of the higher x regimes was the introduction of the concept of Si NCs "touching" that we gained from the study of the high density ($x > x_c$) regime. This enabled us to consider the transport in the present work within the framework that was previously used for granular metals.[8] On the other hand, while this approach is a good starting point, we are well aware that the present system provides a much richer physical arena and possible new applications. The latter originate from the relatively "well separated"-levels of the quantum dots that, unlike the electronic structure in metals, enables (electrically and/or optically) a controllable carrier population of the relevant levels.[21,24,66] Hence, in addition to the charge storage effects, we have here carrier excitation and various "trapping" effects[24] that determine both optical and electrical properties. We note in passing that this difference enables the most significant applications of (dense enough) Si NCs systems, i.e., the LEDs (Ref. 13) and the non-volatile memories.[6]

As the density of the NCs increases in the $x \rightarrow x_d$ regime, the transport mechanism changes to involve the contribution of the tunneling between clusters that are made of touching Si-NCs. The transport in this regime has not been studied at all for ensembles of semiconductor NCs and not, in any detail, even in granular metals. Noting the structure of the NC ensembles as revealed in our HRTEM images it appears, however, that the transport there is still dominated by the tunneling under quantum confinement and Coulomb blockade between individual (non touching) NCs as in the $x \rightarrow 0$ regime.

Coming to the $x \approx x_d$ regime, it appears to be clear now that the role of the inter-cluster tunneling increases with increasing x. In other words, the larger the Si NCs clusters and the larger their concentration, at the expense of the single (non touching) crystallites, the more dominant this tunneling. The study of the properties of the clusters that are made of touching crystallites enables us now to discuss the intermediate-x regimes in terms of a percolation cluster theory.[61,63] Correspondingly, we discovered the "local deconfinement" transition for carriers in general, and for electron-hole pairs, in particular. The latter has been well identified here by the common peak found (at $x = x_d$) in the dependencies of the PL and the SC on the density of the Si NCs. Turning then to the $x_d < x < x_c$ regimes, we can summarize the transport mechanism there as being determined by a combination of the Simanek[40] hopping and the transport mechanism that we concluded (see also below) within the clusters of "touching" NCs. Judging from our own experience in the preparation of the Si NCs/SiO_2 system, the experience gained for granular metals[8,48] and the theoretically predicted dependence of the percolation threshold on the sizes of the particles and the separation of the clusters[110], the resultant behavior of the transport is expected to be very sensitive to details of the structure of the ensembles and thus to the conditions under which the samples were prepared. In particular, we note that for the granular metal of tungsten grains embedded in an Al_2O_3 matrix,[48] a non-monotonic dependence of the conductivity on the metallic content is revealed (as the percolation threshold is approached from the dielectric regime). While no quantitative analysis was given to the corresponding behavior in that work, it is apparent that the formation of larger single grains, at the expense of the formation of more clusters (that may be controlled by proper annealing), can reduce (for x just below x_c) considerably the contribution of these clusters to the transport. This brings about a "sharper" percolation transition that can be well fitted[48] to the predictions of classical percolation theory as given by Eq. (4)[63,109] rather than to the tunneling dominated case as given by the non universal percolation behavior.[65,111]

With further increase of x, the system reaches the close proximity of the percolation threshold. Thus, in addition to the above described inter-clusters conduction, there is now a significant contribution of the percolation cluster that is connected in parallel to the transport via the finite but large clusters. While the situation seems then to be, a priori, even more complicated than the intermediate ($x_d < x < x_c$) density regimes, we saw in our work that the dominant mechanism is relatively easy to follow in this case.[46] This is a consequence of the fact that the percolation cluster may contain a few DBTJs that dominate the conduction path and thus may simplify the understanding of the transport. In turn, we note that the presence of DBTJs provides the so difficult to obtain information on the isolated Si NCs (see above) from macroscopic measurements.[46] In this $x \approx x_c$ regime, we have clearly confirmed the presence of a "voltage gap" and we

have quantitatively determined the charging effects that are similar to those observed in lithographically fabricated single electron transistors.[15] On the other hand, from our results, thus far, we cannot estimate the relative contribution of the Coulomb blockade and quantum confinement. We noted already above that this problem appears to be unresolved also in previous studies of various systems of Si NCs, and thus, until now the effect of the quantum confinement on the transport has not been clearly identified from transport measurements. However, it appears that we do have some indirect evidence for the possible role of the quantum confinement effect on the phototransport properties in this $x \approx x_c$ regime. The evidence for that is the charge polarization effect that we found to be induced in a string of Si NCs with a monotonic change of the crystallites size.[57] In that work, we revealed an anomalous photovoltaic phenomenon for x just above x_c. We interpreted that observation to be due to the interplay between the quantum confinement effect and the Coulomb blockade effect within clusters of Si Ncs, when there is a well defined direction for the size variation of the NCs within the clusters. The model that we suggested for these observations was that the spatial range of the electron-hole separation is determined by the difference between the energy level shifts of the conduction band edge and the valence band edge in the single Si QD (Refs. 26 and 34)) along the string, on one hand, and the electric field build-up that opposes the corresponding charge separation, on the other hand.[57]

In passing, we note that this phenomenon is just one of the special effects that can be obtained in semiconductor QDs and cannot be obtained in granular metals. Another phenomenon that we have observed recently is, that following some specific annealing conditions the Si/SiO_2 composites exhibit long-time (hours) conductivity relaxation and aging effects. These are very similar to those found in some porous silicon structures[116] but for which no specific mechanism was suggested thus far. It will be interesting to further examine these phenomena and find if they are related to electronic glasses out of equilibrium[117] and in particular to those observed recently in granular metals.[118] We note, however, that as in the latter systems, the hopping and charging mechanisms that we described above can provide a basis for the interpretation of these phenomena.

As the density of the Si NCs exceeds the percolation threshold from below, we encounter a situation where there are enough of the Si NCs that "touch" their adjacent neighbors so that the dominant current takes place via a percolation network of "touching" NCs. Our percolation-based conclusion is based on three observations; the actual "structural" touching, the fact that the universal percolation behavior in the continuum is associated here with the onset of a network of "touching" particles, and the finding that the x_c values of the thresholds are between that of the effective medium (EM) value (of a fractional conducting phase content of 33 vol. % (Ref. 63)) and the ~50 vol. % (Refs. 48 and 67) values that are typical of granular metals. Our above conclusion is also supported by the common percolation behavior of both $\sigma_d(x)$ and $\sigma_{ph}(x)$ that we found.[46,61] We note in passing that there are very few works in which a percolation-like transition has been reported for the $\sigma_{ph}(x)$ dependence. The fact that the common parameter of σ and σ_{ph} is the electron mobility, μ, and the fact that both conductivities have the same x dependence suggest that the transitions in σ_d and σ_{ph} are associated primarily with the transport-connectivity aspect rather than with a change in carrier concentration (i.e., the electronic structure) and/or a recombination (carrier life-time) induced mechanism. We note, however, that we detected small deviations from the proportionality of the two conductivities. This suggests that the recombination process is also x-dependent. While these deviations have not been studied yet, it appears that they may serve in principle as a tool for the evaluation of such processes. We further note that the above percolation-like dependence of the photoconductivity also supports a suggestion that was made previously for μc-Si:H (Ref. 119) that the photogenerated carriers that contribute to the phototransport are only those that are generated in the backbone of the percolation network of touching crystallites. Hence, all the above facts support our view that the high-x regime in our samples is similar in its connectivity to the one encountered in granular metals above the commonly known[8,48] percolation threshold. On the other hand, the interparticle conduction mechanism is that of a disordered semiconductor[77] while in granular metals, it is that of disordered metals.[8]

The main tool that we applied for the derivation of the above conclusion regarding the inter-NCs transport in this high x regime was a comparative study of the temperature dependencies of the conductivity and the photoconductivity and the parameters E_a and γ_e that we derived from them. We have seen that, in principle, the four conspicuous mechanisms that may account for the observed $\sigma(T)$ dependence are: thermionic emission over barriers between adjacent semiconductor crystallites,[15,38] thermally activated tunneling,[87,89] variable range or near neighbor hopping,[52,81,108] and temperature induced shift of E_F throughout the landscape of the state distribution in the mobility gap (similar to the one encountered in a-Si:H (Ref. 101)). We note, in particular, that while this last mechanism has not been proposed for ensembles of Si NCs, it was suggested previously for the reminiscent μc-Si:H systems.[120,121]

Trying to decide between these scenarios, we analyzed the observed $\sigma(T)$ and $\sigma_{ph}(T)$ characteristics in some detail, finding that the presentation of these data on a log σ vs. log T scale, yielded a concave dependence. The fact that this dependence was similar for the various sputtered systems that we studied (some with possible potential barriers and some without such barriers), as well as the consideration of the $\sigma(x)$ dependence, enabled us to exclude the two most "popular" mechanisms suggested previously[15] for transport in dense ensembles of Si NCs. These are the hopping between crystallites and the thermionic emission mechanisms. Starting with the latter we have presented three main reasons for the conclusion that the semiconductor-semiconductor-barrier based models do not apply to the system that is the subject of this review. The first is that the observed dependencies of $\sigma(T)$ and $\sigma_{ph}(T)$ are very similar to those observed not only in various microcrystalline[122] and nanocrystalline[38] Si materials, but also in a-Si:H (Refs. 123–125) where there are no apparent barriers in the system. The second reason is that there cannot

be a "double" Schottky barrier-like depletion region in Si NCs that are QDs (as in bulk semiconductors where thermionic emission is well accounted for[37,69,71]), since there are only very few donors (or charges) that may be introduced into a single NC. The third reason is that the distinction between surface and bulk states becomes blurred as the crystallite size becomes less than 10 nm.[70] We can conclude then that in the system of NCs that we studied here a crystallite and its surface form a single electronic entity.

In view of the above, we suggested that in the high-x regime, the narrow separation between touching crystallites provides "only" a local disturbance in the potential landscape over distances that are of the order of the size of the NCs. Again, this picture is supported by the closely related system of μc-Si:H for which there are ample evidence against the role of inter-crystallite barriers that have to be thermally surmounted. These include the estimations of their small heights,[126,127] small widths,[38,128] and negligible effect on the transport.[129] This picture is also consistent with the relatively high mobility values (>1 cm^2/V s) that were determined for μc-Si:H structures.[121,129,130] Correspondingly, we further suggest that the interfaces between the NCs provide only "minor" (low and narrow) potential barriers that act more like scattering centers (e.g., by quantum reflections and/or disturbing local atomic potentials[71]) than thermally surmountable barriers. In other words, the NCS interfaces yield essentially only potential fluctuations, such as defects in crystals or structural imperfections in disordered semiconductors. Turning now to the hopping scenario, we suggest, in view of the presence of band tails in all the above mentioned systems that the transport at very low temperatures[63,66,77] is taking place by hopping. However, this hopping is not between the crystallites as proposed for the $x < x_c$, regime,[39,40] but between the defect states that exist in the NCs, their surfaces and/or the boundaries between them when they touch. The latter conclusion is based on the fact that hopping phenomena become significant only at low ($T < 50$ K) temperatures[77,79] and the fact that there is very little evidence in the literature to support the existence of the various intercrystallite hopping mechanisms for the above liquid-nitrogen temperature range studied here.

Arguing against the barrier and hopping models for $x > x_c$, we propose then that in the high-x regime, we have a continuous disordered network through which the carriers propagate under the effect of the resulting potential fluctuations. As outlined theoretically by O'Leary and Lim,[131] the latter are manifested by a band tail state distribution that is reminiscent (but different in detail) of the Cohen, Fritzsche, and Ovshinsky (CFO) model.[132] To further test this picture, we have examined the dependence of γ_e on temperature, noting that this parameter is known to be sensitive only to the recombination kinetics.[59] Indeed, we found a γ_e(T) behavior that we have shown previously to be associated with recombination in band tails.[68] A strong support to this view comes also from the similarity of the temperature dependence of the photoconductivity found here, and in a-Si, a-Si:H (Refs. 105, 133 and 134) and disordered chalcogenides.[59] In fact, this further suggests that, as in the latter systems, the conduction in the studied system of Si NCs takes place by extended states in a continuous network. Additional support to this interpretation comes from our observation that doping of the Si-NCs system can contribute not only to localized states (as manifested by the corresponding PL (Ref. 135)) but also to the free carrier concentration, as in bulk semiconductors, It is interesting to note that the above result seems, *a priori*, to contradict theoretical expectations[136] of doping only at the NC surface, since the dopant is expected to saturate bonds and thus the carrier that it provides is not expected to contribute to the conduction.[137] Our present results on the 3D ensembles in the high-x regime indicate that this distinction is not valid here, and thus, we attribute our observation to the fact that the carrier provided by the dopant "belongs" to the entire network as in a (ordered or disordered) Si bulk matrix. In turn, this lends further support to our continuous disordered network model. Our findings are consistent then with the model of the shift of the Fermi level within the DOS of a disordered semiconductor, in general, and in a band-tail states landscape in particular.[101,121,129,138] In principle, this was also the view of Hamasaki *et al.*[99] in their interpretation of the temperature dependence of the conductivity in SIPOS which is a Si/SiO_2 system that is quite similar to the one with which we were concerned here. Adopting the above model, we suggest then that the activation energy derived at a given temperature reflects (but is not necessarily equal to) the E_c-E_F separation. Consistent with our results, the effect of doping is then to reduce the values of E_c-E_F and E_c-E_{Fq} for a given landscape of the DOS.

V. SUMMARY

In this review, we followed the evolvement of the transport mechanism with the increase of the ensembles density of Si NCs that are embedded in an insulating matrix. The conclusions derived in this review and the questions that are raised in it are based on our own electrical and optical measurements as well as on a thorough examination of the literature on the transport in such ensembles, other silicon systems and granular metals. The approach we took was primarily to exclude some of the transport scenarios that were proposed and then to suggest the most likely one, while realizing that much more work is necessary in order to obtain more detailed models. The hope is, however, that this review will serve as a framework for future discussions of the transport in the present and in similar systems.

Starting with the very dilute ensembles of Si NCs, the presence of only geometrically isolated individual spherical NCs and the clear optical evidence for a quantum confinement effect, suggest that only inter-NC hopping-like transport mechanism can take place between them. The very few relevant transport data in the literature for that regime can be definitely interpreted on the basis of the Simanek model in which, "resonant tunneling" and the presence of a Coulomb blockade, with distributions of NC sizes and inter-NC distances, are assumed. As the volume fraction of the NCs, x, increases, the transport involves also tunneling between clusters that consist of touching NCs. The concept of touching crystallites developed in our work amounts in practice to crystallites the separation between which is of the order of 0.5 nm. The application of this concept provides a useful tool for the analysis of the whole x range except for the

above mentioned very dilute regime. Indeed, just above the latter regime, we discovered a "local deconfinement" transition for the carriers. This delocalization is manifested by diminishing charge storage and photoluminescence, as the concentration of the non touching NCs is decreased in spite of the increase of x. The transport mechanism there and in the higher x regimes up to the percolation threshold of the network of touching NCs, x_c, is being determined by a combination of the Simanek hopping and the transport mechanism within the clusters of "touching" NCs. The regime just below x_c is, however, the least studied and least understood regime in the present and other similar systems in all of which the relative contribution of the various mechanisms depends strongly on the dispersion of the conducting particles. At $x \approx x_c$, we found the presence of DBTJs that may yield information on the isolated Si NCs from macroscopic measurements. In that regime, we have clearly confirmed the presence of a "voltage gap" and we have quantitatively determined the charging effects that are similar to those observed in lithographically fabricated single electron transistors. On the other hand, from our results thus far, we could not estimate the relative influence of the Coulomb blockade and the quantum confinement on the transport. However, an indication for the presence of both effects is the charge polarization effect that we found to be induced in a string of Si NCs.

The conduction just above the percolation threshold is similar in its connectivity to the one encountered in granular metals above the well known particle-coalescence induced percolation transition. In the $x \gg x_c$ regime, the inter-NCs conduction mechanism is that of a disordered semiconductor rather than by either of the three conspicuous mechanisms that were proposed in the literature for the corresponding transport, i.e., thermionic emission, thermally activated tunneling, and variable range or near neighbor hopping. The picture that we propose then is that in the high-x regime, there is a continuous disordered network in which the carriers are scattered by potential fluctuations. These fluctuations are associated with a band tail state distribution that is reminiscent (but different in detail) of the well known CFO model of disordered semiconductors.

ACKNOWLEDGMENTS

This work was supported in part by the Israel Science Foundation (ISF), in part by the Israeli ministry of Science and Technology and in part by the Enrique Berman chair of Solar Energy Research at the Hebrew University. The author would like to thank M. I. Alonso, I. V. Antonova, D. Azulay, Y. Goldstein, J. Jedrzejewski, O. Millo, A. G. Nassiopoulou, A. Sa'ar, and E. Savir for their valuable contribution to the work reported here.

[1] S. V. Gaponenko, *Optical Properties of Semiconductor Nanocrystals* (Cambridge University press, Cambridge, 1998).
[2] O. Bissi, S. Ossicini, and L. Pavesi, Surf. Sci. Rep. **38**, 1 (2000).
[3] I. Balberg, E. Savir, Y. Dover, O. Portillo-Moreno, R. Lozada-Morales, and O. Zelaya-Angel, Phys. Rev. B **75**, 153301 (2007).
[4] I. Balberg, J. Nanosci. Nanotechnol. **8**, 745 (2008).
[5] I. Antonova, *Electrical Properties of Semi-Conductor Nanocrystals and Quantum Dots in Dielectric Matrix, in Nanocrystals and Quantum Dots of Group IV Semiconductors*, edited by T. V. Torchynska and Yu. V. Vorobiev (ASP, Stevenson Ranch, 2009).
[6] A. G. Nassiopoulou, in *Encyclopedia of Nanoscience and Nanotechnology* (American Scientific, Vlencia-CA, 2004) Vol. **9**, p. 793.
[7] I. S. B. Beloborodov, A. V. Lopatin, and V. M. Vinokur, Rev. Mod. Phys. **79**, 469 (2005).
[8] B. Abeles, P. Sheng, M. D. Coutts, and Y. Arie, Adv. Phys. **24**, 407 (1975).
[9] S. M. Sze and K. K. Ng, *Physics of Semiconductor Devices* (Wiley, Hoboken, NJ, 2007).
[10] *Single Electron Tunneling*, edited by H. Grabert and M. H. Devoret (Plenum, New York, 1991).
[11] C. A. Stafford and S. D. Sarma, Phys Rev. Lett. **72**, 3590 (1994).
[12] S.-K. Kim, C.-H. Cho, B.-H. Kim, S.-J. Park, and J. W. Lee, Appl. Phys. Lett. **95**, 143120 (2009).
[13] N. Daldosso and L. Pavesi, *Low Dimensional Silicon as a Photonic Material, in Nanosilicon*, edited by V. Kumar (Elsevier, Amsterdam, 2008), p. 314.
[14] T. A. Burr, A. A. Seraphin, E. Werwa, and K. D. Kolenbrander, Phys. Rev. B **56**, 4818 (1997).
[15] Z. A. K. Durrani and H. Ahemed, *Nanosilicon Single-Electron Transistors and Memory, in Nanosilicon*, edited by V. Kumar (Elsevier, Amsterdam, 2008), p. 335.
[16] K. Nishiguchi and S. Oda, J. Appl. Phys. **88**, 4186 (2000).
[17] K. Kim, Phys. Rev. B **57**, 13072 (1998).
[18] A. Wan, T. H. Wang, M. Zhu, and C. L. Lin, Appl. Phys. Lett. **81**, 538 (2002).
[19] M. Shalchian, J. Grisolia, G. BenAssayag, H. Coffin, S. M. Atarodi, and A. Claverie, Solid-State Electron. **49**, 1198 (2005).
[20] S. Huang, S. Banerjee, R. T. Tung, and S. Oda, J. Appl. Phys. **94**, 7261 (2003).
[21] M. Fujii, O. Mamezaki, S. Hayashi, and K. Yamomoto, J. Appl. Phys. **83**, 1507 (1998).
[22] M. A. Rafiq, Y. Tsuchiya, H. Mizuta, S. Oda, S. Uno, Z. A. K. Durnani, and W. I. Milne, J. Appl. Phys. **100**, 014303 (2006).
[23] X. Zhou, K. Usami, M. A. Rafiq, Y. Tsuchiya, H. Mizuta, and S. Oda, J. Appl. Phys. **104**, 024518 (2008).
[24] S. Godefroo, M. Hayne, M. Jivanescu, A. Stesmans, M. Zacharias, O. I. Lebedev, G. Van Tendeloo, and V. V. Moshchalkov, Nature Nanotechnol. **3**, 174 (2008).
[25] N. A. Hill and K. B. Whaley, Phys. Rev. Lett. **75**, 1130 (1995).
[26] M. Mahdouani, R. Bourguiga, and S. Jaziri, Physica E **41**, 228 (2008).
[27] O. Millo, D. Katz, Y.-W. Cao, and U. Banin, Phys. Rev. Lett. **86**, 5751 (2001).
[28] M. A. Salem, H. Mizuta, and S. Oda, Appl. Phys. Lett. **85**, 3262 (2004).
[29] T. Feng, H. Yu, M. Dicken, J. R. Heath, and H. A. Atwater, Appl. Phys. Lett. **86**, 033103 (2005).
[30] K. Makihara, J. Xu, M. Ikeda, H. Murakami, S. Higashi, and S. Miyazaki, Thin solid Films **508**, 186 (2006).
[31] O. Y. Raisky, W. B. Wang, R. R. Alfano, C. L. Reynolds, D. V. Stampone, and M. W. Focht, Appl. Phys. Lett. **74**, 129 (1999).
[32] D. L. Klein, R. Roth, A. K. L. Lim, A. P. Alvisatos, and P. L. McEuen, Nature (London) **389**, 699 (1997).
[33] S. Y. Ren and J. D. Dow, Phys. Rev. B **45**, 6492 (1992).
[34] Y. Maeda, Phys. Rev. B **51**, 1658 (1995).
[35] R. E. Chandler, A. J. Houtepen, J. Nelson, and D. Vanmaekelbergh, Phys. Rev. B **75**, 085325 (2007).
[36] Y. M. Niquet, C. Delerue, M. Lannoo, and G. Allan, Phys. Rev. B **64**, 113305 (2001).
[37] J. Y. W. Seto, J Appl. Phys. **46**, 5247 (1975).
[38] Y. He, Y. Wei, G. Zheng, M. Yu, and M. Liu, J. Appl. Phys. **82**, 3408 (1997).
[39] P. Sheng and J. Klafter, Phys. Rev. B **27**, 2583 (1983).
[40] E. Simanek, Solid State Commun. **40**, 1021 (1981).
[41] D. Stielerl, V. L. Dalal, K. Muthukrishnan, M. Noack, and E. Schares, J. Appl. Phys. **100**, 036106 (2006).
[42] S. K. Ram, Md. N. Islam, P. R. i Cabarrocas, and S. Kumar, Thin Solid Films **516**, 6863 (2008).
[43] A. G. Kazanskii, G. Kong, X. Zeng, H. Hao, and F. Liu, J. Non-Cryst. Solids **354**, 2282 (2008).
[44] Y. Lubianiker and I. Balberg, Phys Rev. Lett. **78**, 2433 (1997).
[45] B. Urbach, E. Axelrod, and A. Sa'ar, Phys. Rev. B **75**, 205330 (2007).
[46] I. Balberg, E. Savir, J. Jedrzejewski, A. G. Nassiopoulou, and S. Gardelis, Phys. Rev. B **75**, 235329 (2007).
[47] I. V. Antonova, M. Gulyaev, E. Savir, J. Jedrzejewski, and I. Balberg, Phys. Rev. B **77**, 125318 (2008).

[48]B. Abeles, H. L. Pinch, and J. I. Gittleman, Phys. Rev. Lett. **35**, 247 (1975).
[49]M. I. Alonso, I. C. Marcus, M. Garriga, A. R. Goñi, J. Jedrzejewski, and I. Balberg, Phys. Rev. B **82**, 045302 (2010).
[50]N. Karpov, V. Volodin, J. Jedrzejewski, E. Savir, I. Balberg, Y. Goldstein, T. Egewskaya, N. Shwartz, and Z. Yanovitskaya, J. Optoelectron. Adv. Mater. **11**, 625 (2009).
[51]I. V. Antonova, M. Gulyaev, Z. Sh. Yanovitskaya, V. A. Valodin, D. V. Marin, M. D. Efremov, Y. Goldstein, and J. Jedrzejewski, Semiconductors **40**, 1198 (2006).
[52]M. Fujii, Y. Inoue, S. Hayashi, and K. Yamamoto, Appl. Phys. Lett. **68**, 3749 (1996).
[53]For a review of the structural and optical properties of our samples, see A. Saar, J. Nanophotonics **3**, 032501 (2009).
[54]M. Dovrat, Y. Goshen, I. Popov, J. Jedrzejewski, I. Balberg, and A. Sa'ar, Phys. Status Solidi C **2**, 3440 (2005).
[55]A. Sa'ar, Y. Reichman, M. Dovrat, D. Kraf, J. Jedrzejewski, and I. Balberg, Nanolett. **5**, 2443 (2005).
[56]M. Dovrat, Y. Goshen, J. Jedrzejewski, I. Balberg, and A. Sa'ar, Phys. Rev. B. **69**, 155311 (2004).
[57]H. L. Aharoni, D. Azulay, O. Millo, and I. Balberg, Appl. Phys. Lett. **92**, 112109 (2008); D. Azulay, "Local current routes in ensembles of Si quantum dots" (unpublished).
[58]See for example, D. Azulay, I. Balberg, V. Chu, J. P. Conde, and O. Millo, Phys. Rev. B **71**, 113304 (2005).
[59]R. H. Bube, *Photoelectronic Properties of Semiconductors* (Cambridge University Press, Cambridge, 1992).
[60]I. Balberg, R Naidis, L. F. Fonseca, S. Z. Weisz, J. P. Conde, P. Alpuim, and V. Chu, Phys. Rev. B **63**, 113201 (2001).
[61]I. Balberg, E. Savir, and J. Jedrzewski, J. Non-Cryst. Solids **338-340**, 102 (2004).
[62]I. Balberg, AIP Conf. Proc. **1151**, 5 (2009).
[63]D. Stauffer and A. Aharony, *Introduction to Percolation Theory* (Taylor and Francis, London, 1994); see also I. Balberg, "Continuum Percolation," in *Springer Encyclopedia of Complexity*, edited by M. Sahimi (Springer, Berlin, 2009), Vol. **2**, p. 1443.
[64]For the basic concepts in transport in disordered media see: N. F. Mott and E. A. Davis, *Electron Processes in Non-Crystalline Materials* (Clarendon, Oxford, 1979); B. I. Shklovskii and A. L. Efros, *Electronic Properties of Doped Semiconductors* (Springer-Verlag, Berlin, 1984).
[65]I. Balberg, J. Phys. D: Appl. Phys. **42**, 064003 (2008).
[66]I. Balberg, E. Savir, and J. Jedrzejewski, Phys. Rev. B **83**, 035318 (2011).
[67]I. Balberg, D. Azulay, D. Toker, and O. Millo, Int. J. Mod. Phys. B **18**, 2091 (2004).
[68]I. Balberg, Y. Dover, R. Naides, J. P. Conde, and V. Chu, Phys. Rev. B **69**, 035203 (2004) and references therein.
[69]M. L. Tarng, J. Appl. Phys. **49**, 4069 (1978).
[70]G. Baccarani, B. Ricco, and G. Spadini, J. Appl. Phys. **49**, 5565 (1978).
[71]S. Lombardo, S. U. Campisano, and F. Baroetto, Phys. Rev. B **47**, 13561 (1993). (For the energy level of the oxygen donor see also, V. N. Mordkovich, Sov. Phys. Solid State **6**, 654 (1964).
[72]D. L. Peng, T. J. Konno, K. Wakoh, T. Hihara, and K. Sumiyama, Appl. Phys. Lett. **78**, 1535 (2001).
[73]A. D. Nocera, A. Mittiga, and A. Rubino, J. Appl. Phys. **78**, 3955 (1995).
[74]A. H. Clark, Phys. Rev. **154**, 750 (1967).
[75]A. Lewis, Phys. Rev. Lett. **29**, 1555 (1972).
[76]S. J. Bending and M. R. Beasley, Phys. Rev. Lett. **55**, 324 (1985).
[77]S. R. Elliott, *Physics of Amorphous Materials* (Longman, New York, 1990).
[78]M. L. Ciurea, V. S. Tedorescu, V. Iancu, and I. Balberg, Chem. Phys. Lett. **423**, 225 (2006).
[79]J.-H. Zhou, S. D. Baranovski, S. Yamasaki, K. Ikuta, K. Tanaka, M. Kondo, A. Matsuda, and P. Thomas, Phys. Status Solidi B **205**, 147 (1998).
[80]A. J. Houtepen, D. Kockmann, and D. Vanmaekelbergh, Nano Lett. **8**, 3516 (2008).
[81]S. Banerjee, Physica E **15**, 164 (2002).
[82]M. Berthelot, Ann. Chim. Phys. **66**, 110 (1862).
[83]J. J. Mares, J. Kristofik, and V. Smid, Semicond. Sci. Technol. **7**, 119 (1992).
[84]R. A. Street, Adv. Phys. **25**, 397 (1976).
[85]J. J. Mares, J. Kristofik, J. Pangrac, and A. Haspodkova, Appl. Phys. Lett. **63**, 180 (1993).
[86]D. R. Stewart, D. A. A. Ohlberg, P. A. Beck, C. N. Lau, and R. S. Williams, Appl. Phys. A **80**, 1379 (2005).
[87]M. Kapoor, V. A. Singh, and G. K. Johri, Phys. Rev. B **61**, 1941 (2000).
[88]B. Fisher, K. B. Chashka, L. Patlagan, and G. M. Reisner, Phys. Rev. B **70**, 205109 (2004); See also, S. J. Konezny, M. N. Bussac, and L. Zuppiroli, Appl. Phys. Lett. **92**, 012107 (2008).
[89]P. Sheng, E. K. Sichel, and J. I. Gittleman, Phys. Rev. Lett. **40**, 1 (1978).
[90]J. H. Werner, Solid State Phenom. **37-38**, 213 (1994).
[91]L. I. Glazman and K. A. Matveev, Sov. Phys. JETP **67**, 1276 (1988).
[92]A. I. Yakimov, N. P. Stepina, and A. V. Dvurechenskii, J. Phys. Condens. Matter **6**, 2583 (1994).
[93]D. Popovic, A. B. Fowler, and S. Washburn, Phys. Rev. Lett. **67**, 2870 (1991).
[94]H. F. Wolf, *Semiconductors* (Wiley, New York, 1971).
[95]P. Morgen, U. Hofer, W. Wurth, and E. Umbach, Phys. Rev. B **39**, 3720 (1989).
[96]K. Winer, J. Vac. Sci. Technol. B **7**, 1226 (1989).
[97]T. Kamei and T. Wada, J. Appl. Phys. **96**, 2087 (2004).
[98]*Charge Transport in Disordered Solids, With Applications in Electronics*, edited by S. Baranovski (Weily, Chichester, 2006).
[99]K. Simakawa, J. Non-Cryst. Solids **352**, 1180 (2006); M. Hamasaki, T. Adachi, S. Wakayama, and M. Kikuchi, Solid State Commun. **21**, 591 (1977)
[100]K. Lips, P. Kanschat, D. Will, and W. Fuhs, J. Non-Cryst. Solids **230**, 1021 (1998).
[101]H. Overhof and P. Thomas, *Electron Transport in Hydrogenated Amorphous Silicon* (Springer-Verlag, Berlin, 1989).
[102]R. Vanderhaghen, S. Kasouit, J. Damon-Lacoste, F. Liu, and P. Roca i Cabarrocas, J. Non-Cryst. Solids **338-340**, 336 (2004).
[103]F. T. Reis and I. Chambouleyron, J. Non-Cryst. Solids **299**, 179 (2002).
[104]C. Main, F. Dick, S. Reynolds, W. Gao, and R. A. G. Gibson, J. Non-Cryst. Solids **200**, 263 (1996).
[105]H. Fritzsche, B.-G. Yoon, D.-Z. Chi, and M. Q. Tran, J. Non-Cryst. Solids **141**, 123 (1992).
[106]N. Daldosso, M. Luppi, S. Ossicini, E. Degoli, R. Magri, G. Dalba, P. Fornasini, R. Grisenti, F. Rocca, L. Pavesi, S. Boninelli, C. Priolo, C. Spinella, and F. Iacona, Phys. Rev. B **68**, 085327 (2003).
[107]A. Puzder, A. J. Williamson, J. C. Grossman, and G. Galli, Phys. Rev. Lett. **88**, 097401 (2002).
[108]T. Wang, W. Wei, G. Xu, and C. Zhang, Int. J. Mod. Phys. B **16**, 4289 (2002).
[109]L. F. Fonseca and I. Balberg, Phys. Rev. B **48**, 14915 (1993).
[110]A. Drory, I. Balberg, and B. Berkowitz, Phys. Rev. E **49**, 949(R) (1994).
[111]Z. Rubin, S. A. Sunshine, M. B. Heaney, I. Bloom, and I. Balberg, Phys. Rev. B **59**, 12196 (1999).
[112]R. Wiesendanger, *Scanning Probe Microscopy and Spectroscopy* (Cambridge University Press, Cambridge, 1994).
[113]B. Gross and M. T. de Figueiredo, J. Phys. D: Appl. Phys. **18**, 617 (1995).
[114]J. De la Torre, A. Souifi, M. Lemiti, A. Poncet, C. Busseret, G. Guillot, G. Bremond, O. Gonzalez, B. Garrido, and J. R. Morante, Physica E **17**, 604 (2003).
[115]A. H. M. Kamal, J. Lutzen, B. A. Sanborn, M. V. Sidorov, M. N. Kozicki, D. J. Smith, and D. K. Ferry, Semicond. Sci. Technol. **13**, 1328 (1998). For a very recent work see, P. Manousiadis, S. Gardelis, and A. G. Nassiopoulou, J. Appl. Phys. **109**, 083718 (2011).
[116]S. Borini, L. Boarino, and G. Amato, Phys Rev. B **75**, 165205 (2007).
[117]T. Grenet, J. Dehaye, M. Sabra, and F. Gay, Eur. Phys. J. B **56**, 183 (2007).
[118]N. Kurzweil and A. Frydman, Phys. Rev. B **75**, 020202(R) (2007).
[119]F. Siebke, S. Yato, Y. Hishikawa, and M. Tanaka, J. Non-Cryst. Solids **227**, 977 (1998).
[120]M. Mars, M. Fathallah, E. Tresso, and S. Fenero, J. Non-Cryst. Solids **299**, 133 (2002).
[121]C. E. Nebel, M. Rother, M. Stutzmann, C. Summonte, and M. Heintze, Philos. Mag. Lett. **74**, 455 (1996).
[122]N Pinto, M. Ficcadenti, L. Morresi, R. Murri, G. Ambrosone, and U. Coscia, J. Appl. Phys. **96**, 7306 (2004).
[123]K. Shimakawa and A. Ganjoo, Phys. Rev. B **65**, 165213 (2002).
[124]N. Lustig and W. E. Howard, Solid State Commun. **72**, 59 (1989).
[125]I. P. Zvyagin, I. A. Kurova, M. A. Nal'gieva, and N. N. Ormont, Semiconductors **40**, 108 (2006).
[126]A. Heya, A.-Q, He, N. Otsuka, and H. Matsumura, J. Non-Cryst. Solids **227-230**, 1016 (1998).
[127]Y. Furuta, H. Mizuta, K. Nakazato, T. T. Yong, T. Kamiya, Z. Durrani, H. Ahmed, and K. Taniguchi, Jpn. J. Appl. Phys. **40**, L615 (2001).
[128]F. Diehl, M. Scheib, B. Schroder, and H. Oechsner, J. Non-Cryst. Solids **227**, 973 (1998).

[129]D. Ruff, H. Mell, L. Toth, I. Sieber, and W. Fuhs, J. Non-Cryst. Solids **230**, 1011 (1998).
[130]T. Dylla, F. Finger, and E. A. Schiff, Appl. Phys. Lett. **87**, 032103 (2005).
[131]S. K. O'Leary and P. K. Lim, Solid State Commun. **101**, 513 (1997).
[132]M. H. Cohen, H. Fritzsche, and S. R. Ovshinsky, Phys. Rev. Lett. **22**, 1065 (1969).
[133]Y. Lubianiker, I. Balberg, L. Fonseca, and S. Z. Weisz, Mater. Res. Soc. Symp. Proc. **467**, 209 (1997).
[134]L. Fonseca, S. Z. Weisz, R. Rapaport, and I. Balberg, Mater. Res. Soc. Symp. Proc. **557**, 439 (1999).
[135]M. Fujii, A. Mimura, S. Hayashi, K. Yamamoto, C. Urakawa, and H. Ohta, J. Appl. Phys. **87**, 1855 (2000).
[136]S. Ossicini, E. Degoli, F. Iori, R. Magri, G. Canlele, F. Trani, and D. Ninno, Appl. Phys. Lett. **87**, 173120 (2004).
[137]R.A. Street, Phys. Rev. Lett. **49**, 1187 (1982).
[138]Y. Lubianiker and I. Balberg, Phys. Status Solidi. B **205**, 119 (1997).